



Article

Cite this article: Lovell H, Carrivick JL, King O, Sutherland JL, Yde JC, Boston CM, Matecki J (2023). Surge-type glaciers in Kalaallit Nunaat (Greenland): distribution, temporal patterns and climatic controls. *Journal of Glaciology* 1–18. <https://doi.org/10.1017/jog.2023.61>

Received: 19 January 2023

Revised: 17 July 2023

Accepted: 18 July 2023








Keywords:

Arctic glaciology; glacier surge; ice dynamics

Corresponding author:

Harold Lovell; Email: harold.lovell@port.ac.uk

Surge-type glaciers in Kalaallit Nunaat (Greenland): distribution, temporal patterns and climatic controls

Harold Lovell¹ , Jonathan L. Carrivick² , Owen King³ ,
Jenna L. Sutherland⁴ , Jacob C. Yde⁵ , Clare M. Boston¹  and
Jakub Matecki⁶ 

¹School of the Environment, Geography and Geosciences, University of Portsmouth, Portsmouth, UK; ²School of Geography and Water@Leeds, University of Leeds, Leeds, UK; ³School of Geography, Politics and Sociology, Newcastle University, Newcastle, UK; ⁴School of Built Environment, Engineering and Computing, Leeds Beckett University, Leeds, UK; ⁵Department of Environmental Sciences, Western Norway University of Applied Sciences, Sogndal, Norway and ⁶Institute of Geoecology and Geoinformation, Adam Mickiewicz University, Poznań, Poland

Abstract

We present the first systematic inventory of surge-type glaciers for the whole of Greenland compiled from published datasets and multitemporal satellite images and digital elevation models. The inventory allows us to define the spatial and climatic distribution of surge-type glaciers and to analyse the timing of surges from 1985 to 2019. We identified 274 surge-type glaciers, an increase of 37% compared to previous work. Mapping surge-type glacier distribution by temperature and precipitation variables derived from ERA5-Land reanalysis data shows that the west and east clusters occur in well-defined climatic envelopes. Analysis of the timing of surge active phases during the periods ~1985 to 2000 (T1) and ~2000 to 2019 (T2) suggests that overall surge activity is similar in T1 and T2, but there appears to be a reduction in surging in the west cluster in T2. Our climate analysis shows a coincident increase in mean annual and mean winter air temperature between T1 and T2. We suggest that as glaciers thin under current warming, some surge-type glaciers in the west cluster may be being prevented from surging due to (1) their inability to build-up sufficient mass and (2) a switch from a polythermal to a largely cold-based thermal regime.

Introduction

Glacier surges are flow instabilities that affect ~1% of the global glacier population (Jiskoot and others, 2000; Sevestre and Benn, 2015). The traditional surge cycle is characterised by a long (between ~10 to 100+ years) quiescent phase of low ice flow velocities and gradual mass build-up in the glacier accumulation area, punctuated by a shorter (months to years) active or surge phase of enhanced ice velocities and mass redistribution from higher to lower elevations, typically accompanied by a period of glacier terminus advance (Meier and Post, 1969; Copland and others, 2003; Murray and others, 2003; Benn and others, 2019a, 2019b). The oscillation between slow and fast ice flow experienced by surge-type glaciers makes them valuable sources of information on glacier processes, flow dynamics and instabilities (Benn and others, 2019a). For example, surges have been shown to cause rapid destabilisation and collapse of large marine-terminating glacier systems and ice cap outlet glaciers in the Arctic (McMillan and others, 2014; Sund and others, 2014; Dunse and others, 2015; Strozzi and others, 2017; Willis and others, 2018; Nuth and others, 2019; Haga and others, 2020). At a typically much smaller scale, sudden mountain glacier detachments have been suggested to form part of the continuum of glacier instabilities that includes glacier surges (Kääb and others, 2021).

Switches between slow and fast ice flow during surges have traditionally been viewed as an internal glaciological phenomenon, independent of external (e.g. climatic) forcing (Meier and Post, 1969; Kamb and others, 1985; Murray and others, 2003). However, a close relationship between the distribution of surge-type glaciers and defined climatic envelopes has been established (Harrison and Post, 2003; Sevestre and Benn, 2015) and a changing climate is altering the behaviour and distribution of surge-type glaciers (Benn and others, 2019a). Most theories of surging relate the velocity switches to changes in basal hydrological or thermal conditions (e.g. Kamb and others, 1985; Fowler and others, 2001), which Benn and others (2019a) combine in their enthalpy cycle model. This theory states that a glacier's enthalpy budget (thermal energy and water gains and losses at the glacier bed) takes the form of geothermal heating plus frictional heating due to ice flow (gains) and heat conduction and meltwater discharge (losses). For steady state flow, a glacier's mass and enthalpy budgets need to simultaneously balance, and surge cycles occur where they are out-of-phase (Benn and others, 2019a). In both temperate and polythermal glacier surges, enthalpy gains at the glacier bed result in more meltwater being produced than can be evacuated by the basal drainage system (Sevestre and others, 2015; Benn and others, 2023). The accumulation of water at the bed reduces basal friction, increases

© The Author(s), 2023. Published by Cambridge University Press on behalf of The International Glaciological Society. This is an Open Access article, distributed under the terms of the Creative Commons Attribution licence (<http://creativecommons.org/licenses/by/4.0/>), which permits unrestricted re-use, distribution and reproduction, provided the original article is properly cited.

cambridge.org/jog



sliding speeds and draws down mass from the accumulation area. Surges terminate once basal water storage reaches a high enough level for an efficient drainage system to develop, allowing basal water to be evacuated (Benn and others, 2023). The main distinction between temperate and polythermal surges is that some smaller polythermal surge-type glaciers will only have limited areas of warm-based ice in the quiescent phase. Low ice fluxes result in glacier thickening, with the associated enthalpy gains at the bed leading to progressive basal warming. As the bed warms, the volume of stored water increases, basal friction reduces and the ice accelerates (Fowler and others, 2001; Benn and others, 2023). Larger polythermal glacier surge-type glaciers have been shown to be mainly warm-based apart from a frozen frontal margin, even in quiescence, so thermal switching does not explain surge initiation (Sevestre and others, 2015). However, progressive warming of the frozen frontal zone once the surge is already underway may lead to further acceleration phases (Nuth and others, 2019; Benn and others, 2019b; Haga and others, 2020).

The Benn and others (2019a) general theory of surges helps to reconcile both the distinct geographical clustering of surge-type glaciers within defined climatic envelopes (Jiskoot and others, 2000; Sevestre and Benn, 2015) and the large diversity in surge characteristics (Benn and others, 2023). Most surge-type glaciers are found in a few dense regional groupings, which can be broadly categorised into (1) a circum-Arctic population (termed ‘Arctic Ring’ in Sevestre and Benn (2015)), including Alaska-Yukon (Clarke and others, 1986; Harrison and Post, 2003), the Canadian Arctic Archipelago (Copland and others, 2003; Lauzon and others, 2023), west and east Greenland (Jiskoot and others, 2003; Yde and Knudsen, 2007), Iceland (Björnsson and others, 2003), Svalbard (Jiskoot and others, 2000) and the Russian High Arctic (Grant and others, 2009; Wytiahlowsky and others, 2023); (2) a High Mountain Asia population (Guillet and others, 2022), including the Karakoram (Hewitt, 1969; Quincey and others, 2011; Bhambri and others, 2017), Pamirs (Lv and others, 2019; Goerlich and others, 2020), Tien Shan (Mukherjee and others, 2017) and the Tibetan Plateau (King and others, 2021); and (3) a small population in the Andes (Lliboutry, 1998; Falaschi and others, 2018). Surges occur in continental and maritime environments, in land-terminating and marine-terminating glaciers, under temperate and polythermal glacier regimes and in all glacier sizes from ice sheet outlet glaciers to mountain glaciers.

Compared to surge clusters in other locations (e.g. Alaska-Yukon, Iceland, Svalbard, Karakoram), the distribution, characteristics and timing of surges in Greenland remain poorly documented (Jiskoot and others, 2003). Significant advances have been made over the past few decades, with studies generally focused on a detailed assessment of surging at one or two glaciers (e.g. Colvill, 1984; Jiskoot and others, 2001; Murray and others, 2002; Pritchard and others, 2003, 2005; Yde and Knudsen, 2005; Jiskoot and Juhlin, 2009; Mouginit and others, 2018; Yde and others, 2019; Solgaard and others, 2020) or inventories of individual clusters (west and east Greenland) or groupings (northern Greenland) of surge-type glaciers (e.g. Jiskoot and others, 2003; Yde and Knudsen, 2007; Hill and others, 2017). Sevestre and Benn (2015) represent the most-comprehensive attempt at a Greenland-wide assessment of surge-type glacier distribution since Weidick (1988), albeit as part of a global investigation into surge-type glaciers and thus limited to published reports of surging. In particular, quantitative data on spatio-temporal patterns of surge behaviour are notably lacking in previous work. Newly available and accessible multi-temporal remote sensing datasets present an opportunity to explore the distribution and characteristics of surge-type glaciers across Greenland in more detail. A better understanding of surge-type glaciers in

Greenland can, therefore, provide important information on glacier instabilities in a region that has been experiencing warming air temperatures (e.g. Abermann and others, 2017; Hanna and others, 2021), warming ocean waters (e.g. Murray and others, 2010; Straneo and others, 2012), increasing precipitation (Mernild and others, 2015) and accelerating glacier change (e.g. Khan and others, 2022; Carrivick and others, 2023a).

Our study aims to: (1) produce an updated surge-type glacier inventory for Greenland; (2) provide the first analysis of spatio-temporal patterns of surging in Greenland; and (3) explore the association of glacier geometric properties and regional climate conditions with surge-type glacier distribution.

Surge-type glaciers in Greenland

Surge-type glaciers are predominantly found within the west cluster (Yde and Knudsen, 2007) and the east cluster (Jiskoot and others, 2003), with a small number also located in the southern and northern sectors of the Greenland Ice Sheet (Sevestre and Benn, 2015; Hill and others, 2017) (Fig. 1). Surges have been observed in glaciers and ice caps at the periphery of the Greenland Ice Sheet and large outlet glaciers of the Greenland Ice Sheet itself.

Previous studies identified 89 surge-type glaciers in the west cluster, which extends from 69° N to 71° N and is centred on Qeqertarsuaq (also formerly known as Disko Island) and the Nuussuaq Peninsula (Weidick and others, 1992; Gilbert and others, 2002; Yde and Knudsen, 2007; Citterio and others, 2009; Huber and others, 2020) (Fig. 1). All surge-type glaciers in the west cluster were land-terminating and most were identified on the basis of glaciological (e.g. looped medial moraines, pitted glacier surfaces) or geomorphological (e.g. large moraine complexes) evidence of past surging (Weidick and others, 1992; Yde and Knudsen, 2007). The east cluster covers 68° N to 72° N and the Blossville Kyst, Geikie Plateau and Scoresby Land/Stauning Alper regions (Friese-Greene and Pert, 1965; Henriksen and Watt, 1968; Smart, 1968; Olesen and Reeh, 1969; Rutishauser, 1971; Colvill, 1984; Weidick, 1988, 1995; Woodward and others, 2002; Jiskoot and others, 2003; Walsh and others, 2012) (Fig. 1). The Jiskoot and others (2003) inventory identified 71 glaciers that have been observed to surge or display glaciological evidence for past surge behaviour in the form of looped medial moraines and other diagnostic morphological evidence. Outside of the two main clusters, 18 surge-type glaciers have been reported in the north, south and southwest sectors of the Greenland Ice Sheet (e.g. Koch and Wegener, 1930; Mock, 1966; Weidick, 1988; Higgins, 1991; Weidick and others, 1992; Joughin and others, 1996; Rignot and others, 2001; Palmer and others, 2010; Murray and others, 2015; Hill and others, 2017; Mouginit and others, 2018; Solgaard and others, 2020; Leclercq and others, 2021; Möller and others, 2022) (Fig. 1). The majority are large marine-terminating outlet glaciers, including eight surge-type glaciers draining from the northern sector of the Greenland Ice Sheet between 76° N and 81° N (Hill and others, 2017).

The few studies that have recorded surge characteristics in Greenland indicate significant diversity in the style of surging, with comparisons drawn to the traditional (but restrictive: see Benn and others, 2023) definitions of both ‘Alaskan-style’ (e.g. Kamb and others, 1985) and ‘Svalbard-style’ (e.g. Murray and others, 2003) surges. Information on Greenland surge characteristics (e.g. active phase duration, size of terminus advance, active phase flow velocities, surge cycle length) exists for Kuannersuit Glacier in the west cluster (e.g. Yde and Knudsen, 2005; Yde and others, 2019), Sortebræ and Sermeq Peqippoq in the east cluster (Jiskoot and others, 2001; Pritchard and others, 2005;

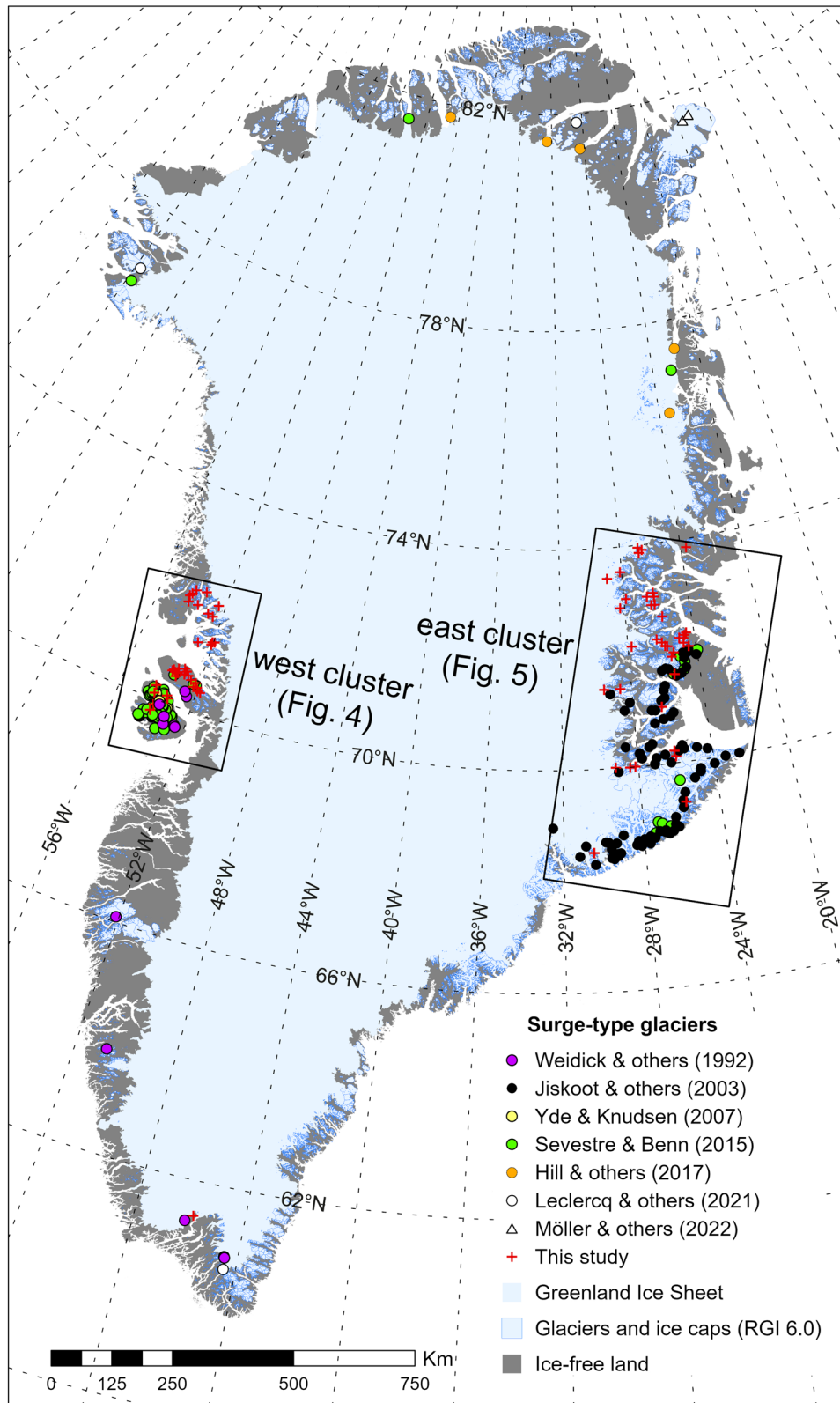


Figure 1. Distribution of surge-type glaciers in Greenland. The symbol for each glacier indicates the references that reported them as a surge-type glacier. See Supplementary Material for the full surge-type glacier inventory.

Jiskoot and Juhlin, 2009), and Hagen Bræ, L. Bistrup Bræ and Storstrømmen in northern Greenland (Reeh and others, 1994, 2003; Mouginit and others, 2018; Solgaard and others, 2020). Based on observations at these glaciers, surge active phase lengths vary from ~3 years (e.g. Jiskoot and others, 2001; Yde and Knudsen, 2005) to up to 10 years (e.g. Rutishauser, 1971; Colvill, 1984; Weidick, 1988; Jiskoot and Juhlin, 2009;

Mouginit and others, 2018; Solgaard and others, 2020). Recorded surge terminus advances ranged from ~3 km (e.g. Jiskoot and Juhlin, 2009; Solgaard and others, 2020) to over 10 km (Reeh and others, 1994; Jiskoot and others, 2001; Yde and Knudsen, 2005). Measured maximum ice velocities/surge propagation rates during the active phase ranged from <math><10 \text{ m d}^{-1}</math> (e.g. Jiskoot and Juhlin, 2009; Mouginit and others, 2018; Solgaard

and others, 2020) to 24 m d^{-1} (Pritchard and others, 2005). Calculated or estimated surge cycle lengths include 20–30 years at Hagen Bræ (Solgaard and others, 2020), 30–50 years at L. Bistrup Bræ (Mouginot and others, 2018), 40–50 years at Sortebræ (Jiskoot and others, 2001) and 70 years at Storstrømmen (Reeh and others, 1994). These few examples of surge characteristics indicate both (1) rapid onset of the surge active phase (Pritchard and others, 2005; Solgaard and others, 2020), short surge duration and high ice velocities (Jiskoot and others, 2001; Pritchard and others, 2005), reminiscent of the traditional definition of ‘Alaskan-style’ surges (e.g. Kamb and others, 1985); and (2) years-long acceleration and deceleration phases, long overall surge duration and lower ice velocities (Jiskoot and Juhlin, 2009; Solgaard and others, 2020; Möller and others, 2022), commonly associated with ‘Svalbard-style’ surges (e.g. Murray and others, 2003; Sund and others, 2014). This demonstrates a wide diversity in Greenland surge behaviour that is consistent with the broad spectrum of glacier surging observed across the other main surge clusters (Benn and others, 2023).

Datasets and methods

Identification of surge-type glaciers

We identified surge-type glaciers in three ways: (1) from details provided in previously published inventories and studies; (2) by visually reviewing optical satellite imagery (Landsat 5 TM, 7

ETM+ and 8 OLI; WorldView via Google Earth; Planet; Esri ArcGIS Pro imagery basemap) for evidence of the surge active phase and glaciological and geomorphological surge features (e.g. Copland and others, 2003; Grant and others, 2009) (Fig. 2); and (3) by using multitemporal difference DEMs (dDEMs) to identify ice surface elevation gains that are substantial and spatially consistent with surge-related mass redistribution (e.g. Lovell and others, 2018; King and others, 2021; Guillet and others, 2022) (Fig. 3). An adapted version of the established three-class surge index (Table 1) was used to categorise glaciers. Surge-type glaciers were given a surge index of 3: observed surge-type glacier (direct evidence of surging, such as an observed surge active phase), 2: probable surge-type glacier (indirect evidence diagnostic of surging, such as looped medial moraines and crevasse-squeeze ridges) or 1: possible surge-type glacier (indirect evidence consistent with surging, such as a pitted glacier surface). All evidence of surging was corroborated by multiple analysts.

Previous surge-type glacier inventories and studies

We established the locations of surge-type glaciers included in previous regional and global inventories (e.g. Weidick, 1988; Weidick and others, 1992; Jiskoot and others, 2003; Yde and Knudsen, 2007; Sevestre and Benn, 2015; Hill and others, 2017; Leclercq and others, 2021; Kääb and others, 2023) and site-specific studies (e.g. Henriksen and Watt, 1968; Rutishauser, 1971; Weidick, 1984; Jiskoot and others, 2001; Murray and others,

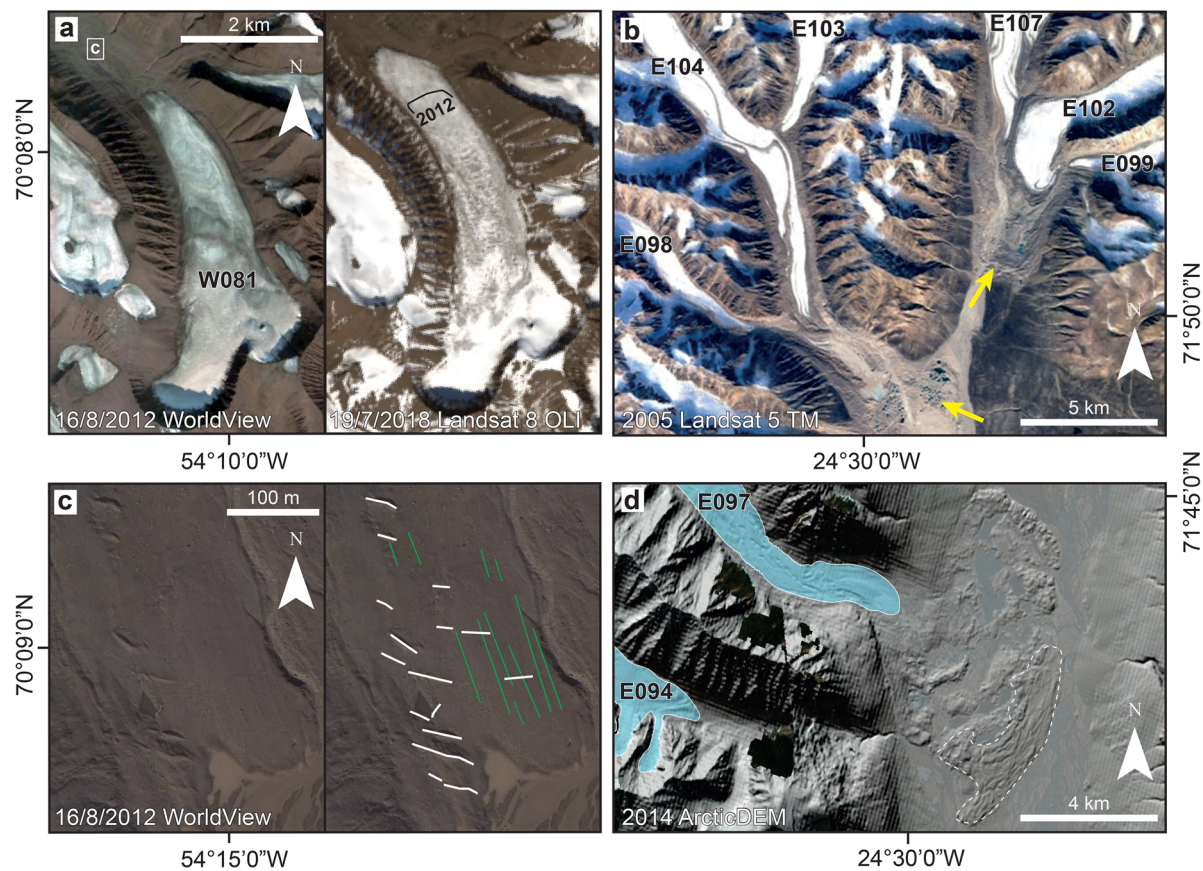


Figure 2. Examples of glaciological and geomorphological evidence used to identify surge-type glaciers. See Supplementary Material, Table S1 for a full list of the surge-type glacier IDs labelled here and more details on each glacier. (a) Terminus advance of glacier W081 (our inventory ID; 1HE11013 in Weidick and others, 1992) during its 2013 to 2018 surge. Left shows the pre-surge WorldView image accessed via Google Earth (16 August 2012) and right shows the surge maximum Landsat 8 OLI image (19 July 2018) with the August 2012 frontal position overlain (black line). (b) Looped and deformed medial moraines on the surface of E104 (Storgletsjer), E107 (Schuchert Gletsjer) and E102 (Sirius Gletsjer). Also shown are surge-type glaciers E098 (Gannochy Gletsjer), E099 (Aldebaran Gletsjer) and E103 (unnamed). Yellow arrows identify prominent proglacial moraine complexes associated with the surge-type glaciers. (c) Crevasse-squeeze ridges (white lines in right panel) and flutes (green lines in right panel) on the foreland of W081 (1HE11013 in Weidick and others, 1992). (d) Glaciotectonic moraine complex (within dashed white line) in front of E097 (Roslin Gletsjer). Also shown is the surge-type glacier E094 (unnamed).

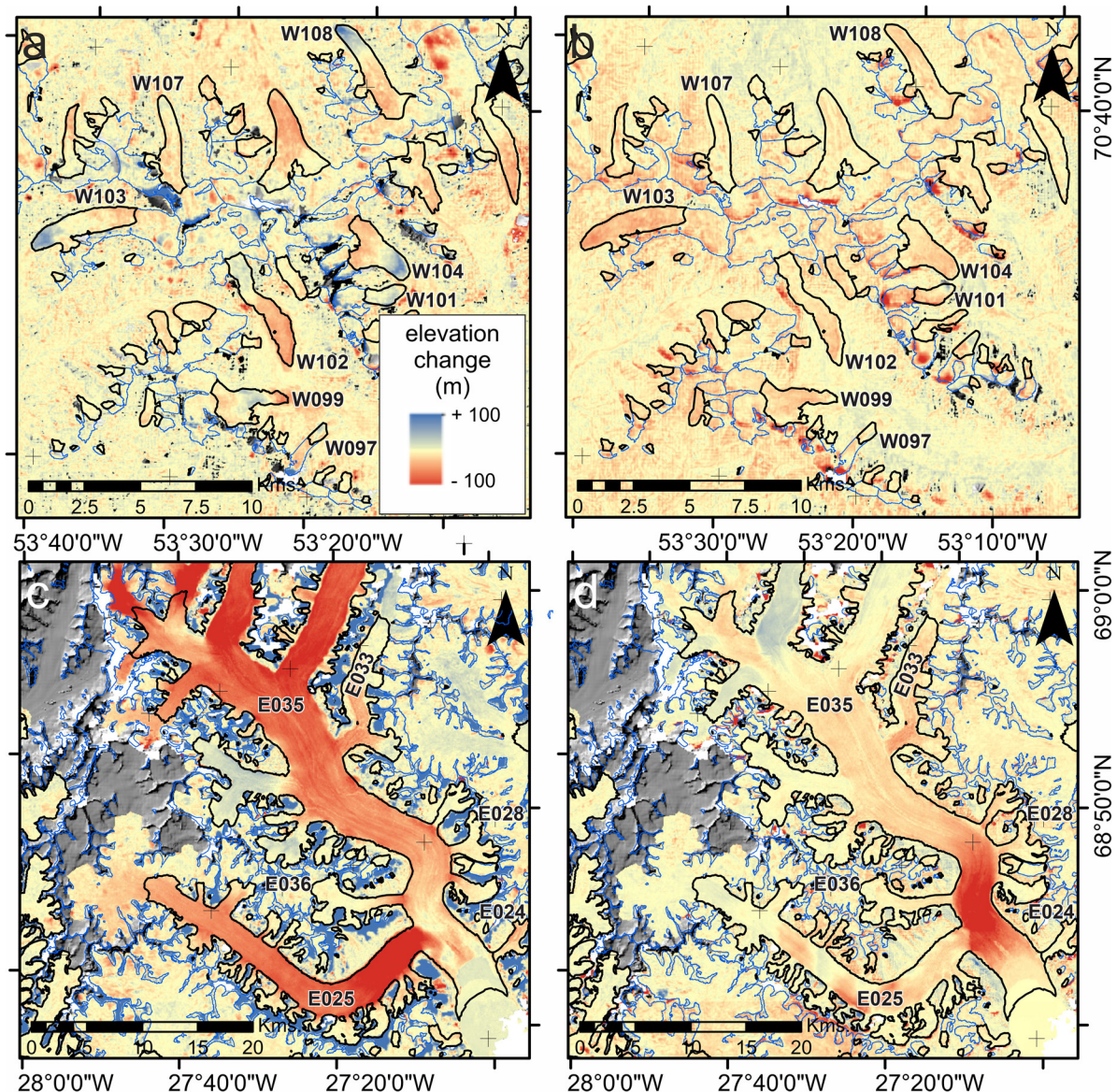


Figure 3. Examples of surges detected using difference DEMs. Surge-type glaciers in our inventory are labelled. (a) Elevation changes of glaciers in western Nuussuaq Peninsula, west cluster, in time one (T1; AeroDEM-GrIMP) and (b) time two (T2; GrIMP-ArcticDEM). (c) Elevation changes within tributary glaciers of Sortebrae, east cluster, in T1 (AeroDEM-GrIMP) and (d) T2 (GrIMP-ArcticDEM). Blue lines are Randolph Glacier Inventory (RGI) 6.0 glacier outlines (RGI Consortium, 2017). Black lines are ablation area outlines. See Supplementary Material, Table S1 for more information on the surge-type glaciers labelled here. Legend in (a) also applies to (b) to (d).

2002; Pritchard and others, 2005; Jiskoot and Juhlin, 2009; Mougnot and others, 2018; Solgaard and others, 2020; Möller and others, 2022). The reported evidence for surge behaviour was assessed and cross-referenced with our own review of satellite imagery and dDEMs and a surge index was assigned (Table 1).

Satellite images

Investigation was primarily focused on the west and east surge clusters (Fig. 1). We visually compared multitemporal Landsat images captured in the 1990s (west Greenland: 1993, 1998, 2000; east Greenland: 1994, 1997, 1998) with recent images (west Greenland: 2017, 2018; east Greenland: 2017, 2018, 2019). Unequivocal surge-related changes (e.g. terminus advance, active deformation of medial moraines) that occurred during this 20–25-year period were recorded, in addition to evidence for past glacier behaviour (e.g. looped medial moraines). Beyond the two main surge clusters, we also reviewed glaciers and ice caps at the periphery of the Greenland Ice Sheet and major outlet glaciers using recent WorldView (accessed via Google Earth), Planet and

Landsat 5 TM, 7 ETM+ and 8 OLI (accessed via Google Earth and Esri ArcGIS Pro basemap) imagery.

Digital elevation models (DEMs)

Multitemporal dDEMs covering two time periods were generated for the west and east surge clusters using three DEM datasets: AeroDEM (dated to 1985 in west Greenland, 1987 in east Greenland), Greenland Ice Mapping Project (GrIMP, based on merged datasets acquired from 2000–2009) and ArcticDEM (2015/2016). AeroDEM (<https://www.ncei.noaa.gov/archive/archive-management-system/OAS/bin/prd/jquery/accession/download/145405>) is a 25 m horizontal resolution digital elevation model derived from aerial photographs (Korsgaard and others, 2016). GrIMP V1 (<https://nsidc.org/data/nsidc-0645/versions/1>) is a 30 m horizontal resolution DEM generated by the integration and enhancement of existing DEM datasets (Howat and others, 2014). ArcticDEM (<https://www.pgc.umn.edu/data/arcticdem/>) is a 2 m horizontal resolution DEM derived using the Surface Extraction with TIN-based Search-space Minimization (SETSM) algorithm applied to WorldView satellite

Table 1. Surge index used to categorise surge-type glaciers in the inventory.

Surge index	Surge likelihood	Evidence	Key references
3	Observed surge-type glacier (direct evidence)	Active phase directly observed (can be current, historical or corroborative), including one or more of the following: terminus advance; measured high flow speeds and changes to velocity profile; surge bulge elevation increases in the ablation zone; chaotic glacier-wide crevassing not explained by other factors; active deformation of medial/frontal moraines.	Meier and Post (1969); Copland and others (2003); Grant and others (2009)
2	Probable surge-type glacier (indirect evidence diagnostic of surging)	Well-preserved surge features, including one or more of the following: looped or deformed medial/frontal moraines; advanced/steep terminus; truncated tributaries/flow-units; crevasse-squeeze ridges; zigzag/concertina eskers; glaciotectionic moraine complexes.	Meier and Post (1969); Sharp (1988); Copland and others (2003); Grant and others (2009); Rea and Evans (2011); Farnsworth and others (2016); Lovell and Boston (2017)
1	Possible surge-type glacier (indirect evidence consistent with surging)	Features characteristic, but not diagnostic of surge behaviour, including one or more of the following: pitted surface; undulating surface; chasms; glacier nailed/proglacial icing; prominent proglacial moraine complex. Includes glaciers in previous inventories/studies for which no evidence for their classification as surge-type was provided or apparent from this study.	Rucklidge (1966); Meier and Post (1969); Weidick (1988); Copland and others (2003); Yde and Knudsen (2007); Grant and others (2009)

Adapted from established surge classifications (e.g. Clarke and others, 1986; Hamilton and Dowdeswell, 1996; Jiskoot and others, 2000, 2003; Copland and others, 2003; Sevestre and Benn, 2015).

images (Noh and Howat, 2015; Porter and others, 2018). In this work we have used the merged ArcticDEM elevation dataset and take it as a representation of glacier surface topography around 2015, which is the most predominant acquisition date of individual DEM strips. We also used the Hugonnet and others (2021) ASTER dDEM time series (2000 to 2009 and 2009 to 2019), which have a 100 m horizontal resolution, to extend our time series towards the present day and provide maximum coverage.

As our study areas cover $\sim 185\,000\text{ km}^2$, DEMs were resampled to a 35 m grid size to streamline processing. The different DEMs were generated from imagery acquired by different sensors and mismatches in their geolocation were evident and required correction. The methods of Nuth and Kääb (2011) were followed to co-register stable (off-glacier) areas and resolve DEM misalignment. Each DEM was split into $5 \times 3\text{ km}$ subsets for this process to allow for the better correction of spatially variable aspect and elevation related biases.

Once co-registered, DEMs were subtracted from one another to derive surface elevation change estimates for the two study areas. We discarded dDEM data above an elevation of 1550 m in the west cluster study area as blunders in DEMs (owing to poor surface contrast in imagery) were prevalent above this elevation. We followed the same approach above an elevation of 1700 m for the east cluster study area. Given most of the glaciers in the study areas sit below these two elevations, this approach did not result in substantial loss of coverage. We also removed estimates of elevation change outside of the range $\pm 150\text{ m}$ under the assumption that these values represented anomalies, rather than real surface elevation change. While some large surges of peripheral Greenland glaciers have resulted in elevation changes greater than this $\pm 150\text{ m}$ range (e.g. Huber and others, 2020), a sufficient portion of each glacier's surge-related elevation gain (thickening) signal was still preserved to allow identification. To establish a suitable level of detection, outside of which we examined the characteristics of elevation changes over glacier surfaces, we firstly examined elevation changes over stable ground surfaces. We generated a mask of stable ground by removing glacier areas (provided by Randolph Glacier Inventory (RGI) 6.0) and glacial lake surfaces in the DEM, and the coastline. We removed elevation differences over stable ground outside of the range $\pm 100\text{ m}$ under the assumption that these data were the result of DEM errors. The standard deviation of remaining stable ground pixels ($n = 17\text{--}53$ million depending on study site and time period) was used as a guide of the remaining variance in elevation data

Table 2. Characteristics of off-glacier surface elevation change estimates following DEM and dDEM post-processing.

dDEM datasets	Mean and SD of the off-glacier dDEM grid (m)
west AeroDEM-GrIMP	-2.3 ± 11.9
west GrIMP-ArcticDEM	-0.1 ± 10.4
west AeroDEM-ArcticDEM	-1.0 ± 10.2
east AeroDEM-GrIMP	-4.0 ± 19.3
east GrIMP-ArcticDEM	0.8 ± 12.5
east AeroDEM-ArcticDEM	-4.3 ± 19.5

(Table 2), outside of which were robust changes in glacier surface elevation.

Surge-type glacier identification using the dDEM datasets focused on the assessment of surface thickening in glacier ablation areas (Fig. 3). We chose to focus primarily on elevation gain in ablation areas because (1) thickening in the lower reaches of a glacier in a region experiencing long-term glacier mass loss, and in established surge clusters, is evidence of the surge active phase (e.g. Citterio and others, 2009; Bolch and others, 2013; Gardner and others, 2013; Carrivick and others, 2017, 2019; Huber and others, 2020); and (2) attributing elevation changes in glacier accumulation areas to surges can be very problematic due to DEM artefacts caused by snow cover in the source satellite or aerial images. Glacier ablation areas were determined by DEM hypsometric analysis using a modification of the Pellitero and others (2015) tool to output a glacier-specific ablation area (as a polygon) (Fig. 3). We specified an area-altitude balance ratio (AABR) of 2.2 for the ablation area analysis following that determined for Arctic glaciers by Rea (2009). In a test on a subset of glaciers, we determined the sensitivity of the ablation zone to the AABR value, finding that a value of 2.3 or 2.1 only altered the ablation area by $<5\%$. We consider the AABR approach to be the best option for providing simple and standardised glacier ablation areas compared to alternative methods that use climate and mass balance conditions. It is possible that ablation areas derived using our approach may be under- or overestimated in cases where the glacier geometry (as defined by RGI 6.0) captures the glacier size at either the start or end of a particular surge cycle. However, given we are only using ablation areas as a simple way to ensure we do not consider elevation changes in the upper parts of glaciers where DEM errors may be larger, we do not think this decision has a major impact on our overall analysis.

Our approach to identifying surge active phases means it is possible we may have failed to identify some surge-type glaciers

using dDEMs, in particular (1) glaciers in the quiescent phase of the surge cycle, characterised by substantial thickening in the accumulation area (e.g. Melvold and Hagen, 1998; Guillet and others, 2022); and (2) marine-terminating glacier surges, where increased mass flux to the ablation area has been compensated by increased frontal ablation, and therefore the elevation gain signature may be muted. However, it is important to note that dDEM signatures are only part of the evidence for surging that we considered in our analysis. For example, marine-terminating glacier behaviour in east Greenland has been extensively studied since the 1980s (e.g. Jiskoot and others, 2012; Walsh and others, 2012; Brough and others, 2023), providing a detailed alternative source of information on potential surging in the region.

Inventory compilation

The locations of surge-type glaciers in the inventory are represented as glacier outlines (from RGI 6.0) and points (based on Global Land Ice Measurement from Space (GLIMS) points and typically located at the centre point of RGI outlines). In cases where independent surge activity has been identified in a tributary or flow-unit within glaciers captured as a single outline in RGI 6.0, we have manually edited the glacier outlines. All glaciers in the inventory have been assigned a unique inventory ID, an RGI ID and a GLIMS ID (Supplementary Materials, Table S1), with the exception of some large ice sheet outlet glaciers ($n=20$) that do not have an RGI outline (and therefore could not be assigned an RGI ID). Our unique inventory ID contains the cluster name (e.g. 'W' for west) followed by three digits organised by increasing latitude within each cluster (e.g. 'W001' is the southernmost surge-type glacier in the west cluster). Where RGI outlines have been edited into separate tributaries/flow-units, the original RGI ID is used with the addition of 'part of'. In cases where GLIMS IDs were absent or could not be identified (e.g. for some large ice sheet outlet glaciers or edited RGI outlines), we have added new GLIMS IDs at appropriate locations following the naming conventions stipulated by RGI Consortium (2017) and adopted by others (e.g. Jiskoot and others, 2012). Glacier names are taken from the Björk and others (2015) database and from previous inventories and studies. Where surge activity is identified within tributaries/flow-units of a larger named trunk glacier, the main glacier name is used followed by an appropriate locational identifier (e.g. 'Glacier name W tributary' for tributaries or 'Glacier name W' for major flow-units). Glacier type and terminus type have been manually assessed using GLIMS glacier classification terms (Rau and others, 2005), with the addition of a subdivision of outlet glaciers into ice sheet (IS) and ice cap/field (IC/F). Glacier areas are derived from the RGI glacier outlines (original and edited) or published sources where there are no RGI outlines (e.g. Weidick and others, 1992; Palmer and others, 2010; Hill and others, 2017; Krieger and others, 2020). The reported evidence for surging and the source of this information is provided for each glacier in the inventory (see Supplementary Materials, Table S1 and GIS files). Here, our surge index (Table 1) is reported alongside the RGI surging status (1 = possible, 2 = probable, 3 = observed, 9 = not assigned), which is based on data used in Sevestre and Benn (2015).

Assessment of spatio-temporal patterns of surging

Information on surge timing fits two categories: (1) well-constrained dates for a surge active phase, either from the literature or observed on satellite images (e.g. dates of terminus advance phases; Fig. 2a); and (2) broadly constrained evidence of a surge

active phase, e.g. identification of ablation area elevation gains in dDEM datasets (Fig. 3) or terminus advance between two image acquisitions (but without exact years of the start and end of the surge active phase). Hereafter we summarise these together as *surge activity* for ease of reporting, which we define as evidence that a glacier is undergoing/has undergone a surge active phase during the period of observation (since ~1985). Surge-type glaciers were then organised into two generalised time periods of approximately the same length based on the dDEM datasets: T1, encompassing the AeroDEM-GrIMP time period (~1985 to 2000; ~15 years); and T2, encompassing the GrIMP-ArcticDEM and ASTER time periods (~2000 to 2019; ~19 years). These time periods are deliberately crude for the purposes of data simplification; for example, we acknowledge that using 2000 for the end/start point of the GrIMP dataset ignores that this is a composite dataset spanning several years (likely 2000 to 2009; Howat and others, 2014). Where surge activity occurs in or spans both periods, the glacier has been counted in each. These generalised time periods allow us to explore spatio-temporal patterns of surging at the scale of the entire surge-type glacier population.

Climate analysis using ERA5-land reanalysis data

To better understand the link between climate and the distribution of surge-type glaciers, we generalised the climate over Greenland and compared our surge inventory to the surface variables from the ERA5-Land dataset generated using a regional climate model (Muñoz-Sabater, 2019) and forced with reanalysis data (Hersbach and others, 2020). The reanalysis product is obtained by combining model data with observations to generate a globally consistent set of meteorological variables that is gap free in space and time. We generated climate variables covering the whole period of study (1981–2020) and for the time periods approximately corresponding to T1 (1981–2000) and T2 (2001–2020) used in the assessment of spatio-temporal patterns of surging. Monthly averaged 2 m air temperature and total precipitation were extracted from ERA5-Land data at $0.1^\circ \times 0.1^\circ$ horizontal grid resolution and processed to compute decadal averages, and for decadal summer and decadal winter means where those seasons were defined for Greenland following Berdahl and others (2018) using June–August (JJA) and December–February (DJF), respectively. We specifically considered mean summer air temperature (T_s) and mean winter precipitation (P_w) in our analyses since these two meteorological variables are important drivers of glacier mass balance (e.g. Mernild and others, 2011). Our climate analyses show positive trends in mean annual air temperature (T_a) and a minor increase in mean annual precipitation (P_a) over the 40-year time period across Greenland, which is consistent with other previous assessments of long-term climate records showing widespread warming and stochastic precipitation patterns (Mernild and others, 2014, 2015; Wong and others, 2015; Westergaard-Nielsen and others, 2018; Finger Higgins and others, 2019; Lewis and others, 2019). In our data, P_a increased by approximately 29.62 mm a^{-1} between T1 and T2 at a rate of $7.4 \text{ mm per decade}$ (for context, P_a ranges from ~200 to ~2500 mm a^{-1} in the period 1981–2020). T_a increased by approximately 2.4°C between T1 and T2 at a rate of $0.6^\circ\text{C per decade}$. These trends are consistent with Wong and others (2015), who state that mean annual temperatures have increased 1.5°C since weather observations in northwest Greenland began in 1952, with a greater increase of 2.7°C from 1981–2012. This pattern was found to be consistent across the whole of Greenland. Statistical analysis of the climate data was performed using Mann-Whitney U tests applied to the west and east clusters at the 95% confidence level.

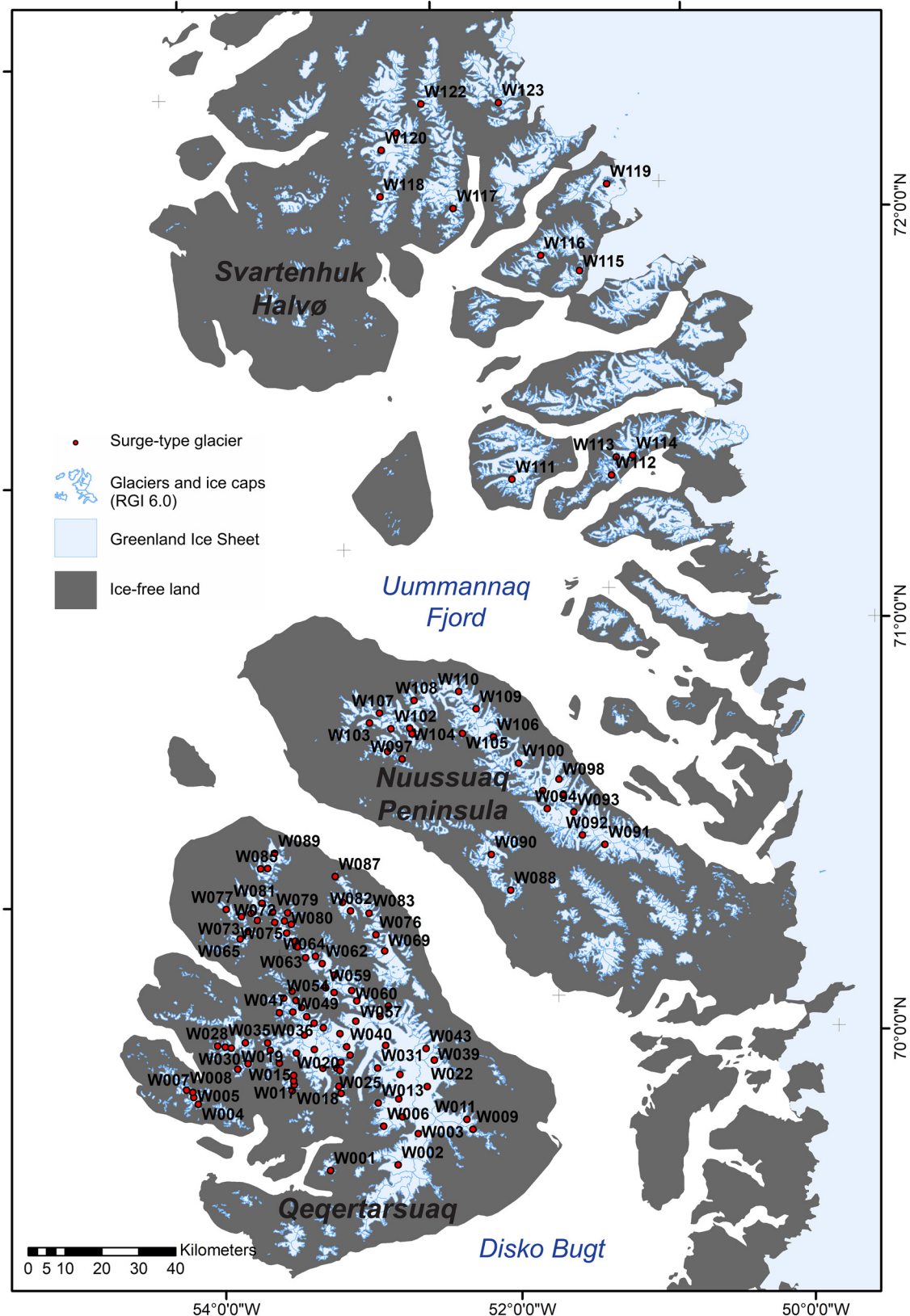


Figure 4. West Greenland surge cluster. See [Figure 1](#) for cluster locations and full surge-type glacier distribution. More information on the surge-type glaciers labelled here can be found in the Supplementary Materials, Table S1.

Results

Greenland surge-type glacier inventory

Our inventory contains 274 surge-type glaciers ([Figs 1, 4 and 5](#), [Table 3](#) and Supplementary Materials, Table S1). This equates to ~1.2% of all glaciers in Greenland, of which there are

>22 000 glaciers and ice caps at the periphery of the Greenland Ice Sheet in RGI 6.0 (Rastner and others, 2012; RGI Consortium, 2017) and >200 major marine-terminating outlet glaciers of the Greenland Ice Sheet (Moon and others, 2012). We have added 74 (+37%) surge-type glaciers not reported in previous inventories or studies: 37 in the west

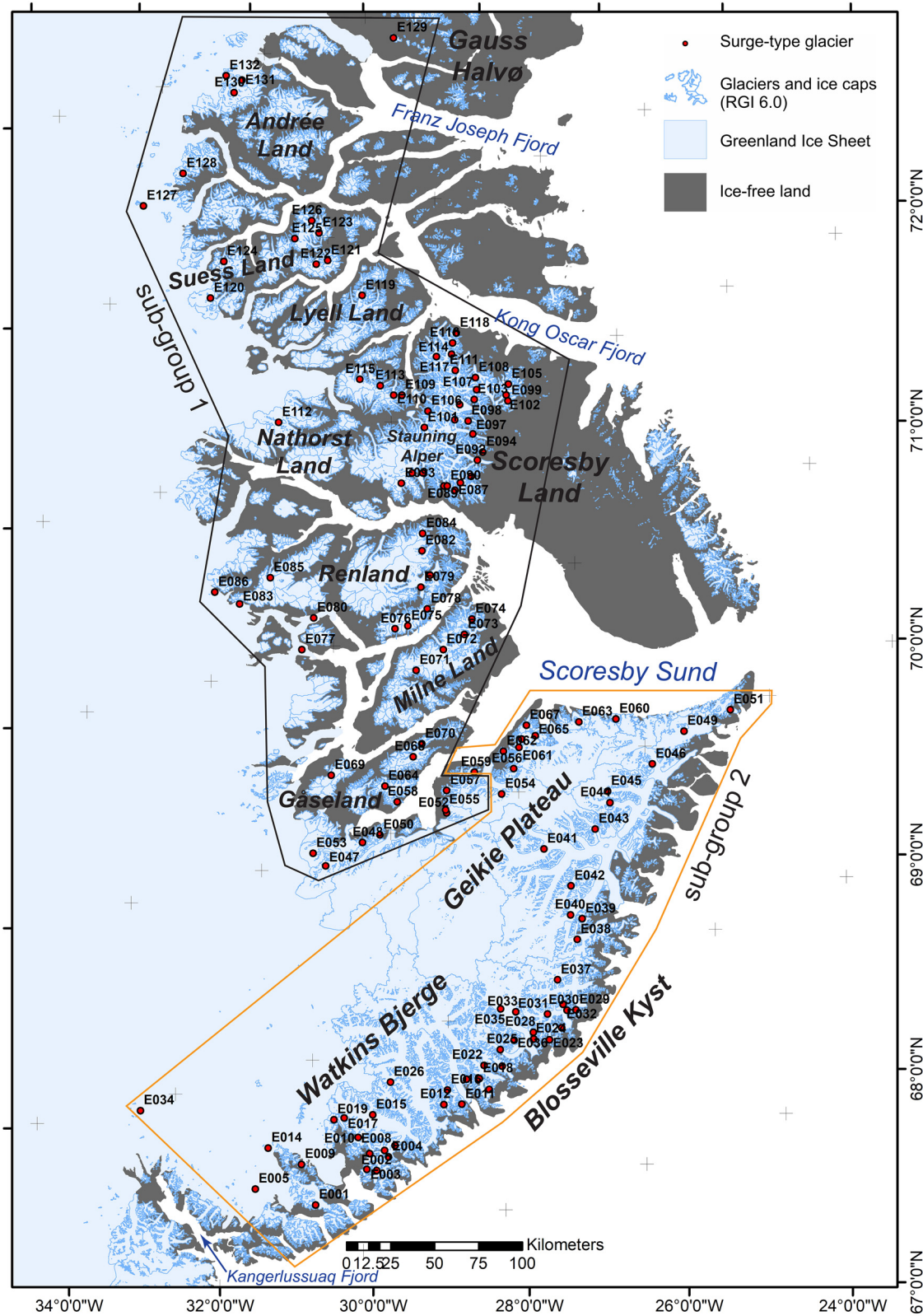


Figure 5. East Greenland surge cluster. See text for reference to east cluster sub-group 1 (black outline) and sub-group 2 (orange outline). See Figure 1 for cluster locations and full surge-type glacier distribution. More information on the surge-type glaciers labelled here can be found in the Supplementary Materials, Table S1.

cluster, 36 in the east cluster and 1 in southern Greenland (Table 3 and Supplementary Materials, Table S1). Of the 74 newly identified surge-type glaciers, 52 have a surge index of 3 (observed surge-type glacier) and 22 have a surge index of 2 (probable surge-type glacier).

Most of the surge-type glaciers are in the west cluster ($n = 123$; 45% of the inventory) (Fig. 4) and the east cluster ($n = 132$; 48% of

the inventory) (Fig. 5). Surge-type glaciers are predominantly valley glaciers or outlet glaciers from ice caps or icefields ($n = 229$; 84%), with very few mountain glaciers identified as being of surge-type ($n = 12$; 4%). The surge-type glaciers we have identified mainly terminate on land ($n = 220$; 80%), including all surge-type glaciers in the west cluster and 71% of surge-type glaciers in the east cluster (Table 3). We identify two geographical sub-groups

Table 3. Summary of all Greenland surge-type glaciers in our inventory (surge index of 1, 2 and 3)

	Clusters/regions				Total
	south	west	east	north	
Surge-type glaciers	7	123	132	12	274
<i>Surge index = 3 (observed)</i>	1	49	67	10	130
<i>Surge index = 2 (probable)</i>	1	44	63	0	105
<i>Surge index = 1 (possible)</i>	5	30	2	2	39
Glacier type					
<i>Outlet (IS)</i>	5	1	17	8	31
<i>Outlet (IC/F)</i>	2	50	56	4	112
<i>Valley</i>	0	60	59	0	119
<i>Mountain</i>	0	12	0	0	12
<i>Surge-type tributary/flow-unit within a larger glacier system</i>	0	6	39	2	47
Terminus type					
<i>Marine</i>	5	0	35	11	51
<i>Land</i>	2	123	94	1	220
<i>Lake</i>	0	0	3	0	3
Surge-type glacier median area (km ²)	94.9	7.8	51.8	4121.0	25.1
Surge-type glaciers included in previous inventories/studies	6	86	96	12	200
New surge-type glaciers identified in this study	1	37	36	0	74

IS, ice sheet; IC/F, ice cap/icefield.

The values show the number of glaciers in each category. See Figures 1, 4 and 5 for distribution and Supplementary Materials, Table S1, for the full inventory. See Table 1 for surge index definition.

within the east cluster (Fig. 5): sub-group 1 surge-type glaciers are mostly located to the north of Scoresby Sund (e.g. Henriksen and Watt, 1968; Rutishauser, 1971; Woodward and others, 2002) and sub-group 2 surge-type glaciers are found in the Blossville Kyst/Geikie Plateau region (e.g. Jiskoot and others, 2001, 2003). The majority of the surge-type glaciers in the east cluster sub-group 1 terminate on land ($n = 66$; 88% of surge-type glaciers in the sub-group). By contrast, most ($n = 29$; 83%) of the marine-terminating surge-type glaciers in the east cluster are found in sub-group 2. Of the 19 surge-type glaciers in southern and northern Greenland, which comprise 7% of the total inventory, 13 are marine-terminating outlet glaciers of the Greenland Ice Sheet (Fig. 1; Table 3). In northern Greenland, over a third ($n = 8$) of the 21 major marine-terminating Greenland Ice Sheet outlet glaciers in the region are surge-type glaciers (Hill and others, 2017). Overall, 130 (47.4% of the inventory) surge-type glaciers have a surge index of 3, 105 (38.3% of the inventory) have a surge index of 2 and 39 (14.2% of the inventory) have a surge index of 1 (Tables 1 and 3).

Newly identified surge-type glaciers show that the west cluster extends northwards onto Svartenhuk Halvø at 72° N (Fig. 4) and the east cluster extends up to Franz Joseph Fjord and Gauss Halvø at 73° N (Fig. 5). A larger proportion of the total number of glaciers in the west cluster are surge-type glaciers (5.2%) than in the east cluster (1.9%). The east cluster also contains 17 ice sheet outlet glaciers and 35 marine-terminating glaciers (13 and 27% of all surge-type glaciers in the east cluster, respectively), largely on the Blossville Kyst (Fig. 5). Surges typically impact a large portion of an individual glacier's area in the west cluster (e.g. Figs 3a and b), where most glaciers have simple configurations characterised by single trunks fed by at most two to three basins. By comparison, in the larger, often multi-branched glaciers in the east cluster, independent surges can occur in several different tributaries or flow-units of the same glacier system (e.g. Figs 3c and d). In these cases, we have identified each surging tributary/flow-unit as a separate surge-type glacier in our inventory to reflect independent surge behaviour. For example, Sortebræ is a large multi-branched surge-type glacier system within which we identify six independent surge-type tributaries or flow-units (E024,

E025, E028, E033, E035, E036) (Fig. 5 and Supplementary Materials, Table S1). Similarly, we identify four independent flow-units within Dendritgletsjer (E040, E041, E042, E043) (Fig. 5 and Supplementary Materials, Table S1). In the few examples like these, we calculate that we have identified 12 additional surge-type glaciers that are recognised as being part of other surge-type glacier systems as mapped by Jiskoot and others (2003) – one-third of the additional surge-type glaciers we have identified in the east cluster (+36) compared to previous work.

Geometric attributes

Compared to the nonsurge-type glaciers (hereafter 'other') in the west and east clusters, surge-type glaciers have larger median areas (west: surge-type glaciers = 7.8 km², other = 0.4 km²; east: surge-type glaciers = 51.8 km², other = 0.5 km²) and greater median lengths (west: surge-type glaciers = 5556 m, other = 774 m; east: surge-type glaciers = 15 418 m, other = 965 m) (Figs 6a and b). Surge-type glaciers also have larger median elevation ranges (west: surge-type glaciers = 861 m, other = 327 m; east: surge-type glaciers = 1700 m, other = 398 m) than other glaciers (Fig. 6c). Surge-type glaciers generally have shallower slopes than other glaciers in both clusters (west medians: surge-type glaciers = 15.6°, other = 19.6°; east medians: surge-type glaciers = 14.4°, other = 20.6°) (Fig. 6d). Using the same geometric data to compare between the two clusters, surge-type glaciers in the east cluster have larger areas, are longer, and have larger elevation ranges than surge-type glaciers in the west cluster (Fig. 6). We find that this is not simply a function of regional differences in glacier size: While there are certainly many more large, multi-branched glaciers in the east compared to the west, there are also many more glaciers overall (west = 2382 glaciers, east = 6863 glaciers), and many of these are very small. This makes the overall glacier size distribution in the east very similar to that in the west, with slightly larger glaciers in the east (reported here as median (interquartile range)): area = 0.4 km² (1.6 km²) in the west; 0.5 km² (2.1 km²) in the east; length = 826 m (1561 m) in the west, 988 m (1879 m) in the east; elevation range = 348 m (474 m) in the west, 408 m (555 m) in the east. Surface slopes of surge-type glaciers (medians = 15.6° and 14.4° in west and east, respectively) and all glaciers (medians = 19.2° and 20.5° in west and east, respectively) are similar in both clusters.

Spatio-temporal patterns

The overall number of glaciers displaying surge activity (evidence of the surge active phase) was broadly similar in T1 ($n = 77$) and T2 ($n = 85$) (Fig. 7a). However, some disparity between T1 and T2 is apparent in the west cluster, where the number of glaciers displaying surge activity is lower in T2 ($n = 25$) than in T1 ($n = 30$). This reduction in surge activity appears particularly clear once the counts of the number of glaciers displaying surge activity are normalised by the differing lengths of the time periods (15 years for T1, 19 years for T2) (Fig. 7b). To explore whether this reduction could be biased by our approach of using the uneven time periods defined by our dDEM datasets, we also adjusted the lengths of the time periods (and the count of surge activity accordingly) to an even 17 years (e.g. 1985–2002 and 2002–2019). This returns a similar reduction in the number of glaciers surging in T2 compared to T1 in the west cluster.

The latitudinal range of surge activity in T1 and T2 was fairly similar, with a slightly smaller latitudinal range in T2 in the west cluster and surge activity extending slightly further north in T2 in the east cluster (Fig. 7c). Across all surge-type glaciers, from T1 to T2 the number of ice sheet outlet glaciers (+7) and ice cap/icefield outlet glaciers (+7) showing surge activity increased, while the

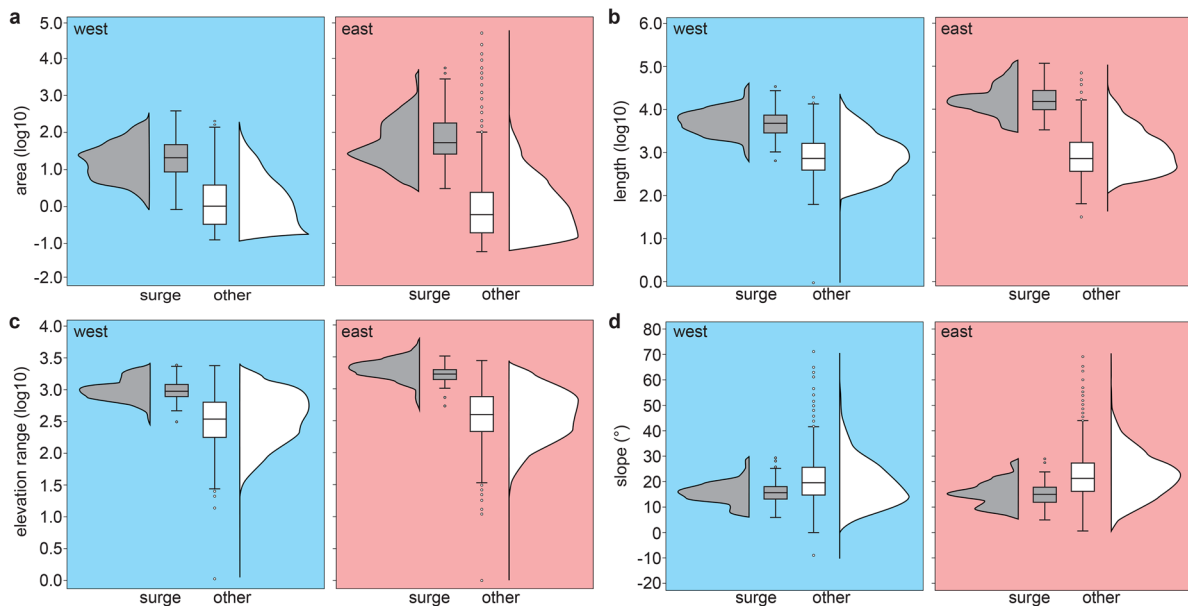


Figure 6. Geometric attributes of all surge-type and nonsurge-type (other) glaciers in the west and east clusters. (a) Area. (b) Length. (c) Elevation range. (d) Slope. Common logarithm (\log_{10}) values are used for area, length and elevation range in order to compare the wide range in values. Geometric attributes are derived from RGI 6.0 (RGI Consortium, 2017), the GLIMS glacier database (Jiskoot, 2002; used for glacier areas of some large glaciers in east Greenland not found in RGI 6.0) or Brough and others, 2023 (used for glacier areas of some large glaciers in east Greenland where no RGI 6.0 or GLIMS outlines exist). The area plot contains all surge-type glaciers in the west ($n = 123$) and east ($n = 132$) clusters. The length, elevation range and slope plots only show surge-type glaciers with RGI 6.0 outlines (west: $n = 119$; east: $n = 99$). We include all categories of surge-type glaciers (surge index of 1, 2 and 3; see Table 1) in our analysis and note that the glacier geometric attributes may not be representative of the conditions at each glacier at the time it surged.

number of valley glaciers (-8) showing surge activity decreased (Fig. 7c).

Climatic distribution

Most surge-type glaciers in Greenland are found within a climatic envelope defined by T_a of -5 to -20°C and P_a of ~ 200 – 1200 mm (Fig. 8a). The only surge-type glaciers found where the climate is warmer and wetter are in the south ($n = 5$). No surge-type glaciers are found where T_a is $> -5^\circ\text{C}$ and P_a is $> \sim 1700$ mm (Fig. 8a). The geographical groupings of surge-type glaciers in Greenland can be resolved into climatic envelopes (Figs 8a and b). The west and east cluster form well-defined climatic envelopes (Figs 8a–f) that are distinct from each other at a statistically significant level for all climate variables (Table 4). West cluster surge-type glaciers are found in a narrow P_a and P_w range ~ 400 – 500 mm and between -13 and -6°C T_a and 0 and 5°C T_s (Figs 8a and b). The east cluster surge-type glaciers cover a larger range in climate conditions than the west cluster and the identified geographical sub-groups (Fig. 5) are distinct from each other at a statistically significant level for all climate variables in the period 1981–2020 (Figs 8a and b), and for P_a and T_a (Figs 8g and i) but not P_w and T_s (Figs 8h and j) when the data are broken down into T1 and T2 (Table 4). An examination of the climate data by time periods also reveals that between T1 and T2 the west cluster surge-type glaciers experienced statistically significant warming of $\sim 1^\circ\text{C}$ for both T_a and T_s (Table 4). Statistically significant T_a warming between T1 and T2 is also found in the east cluster. No statistically significant changes in precipitation (P_a or P_w) between T1 and T2 are found in either cluster (Table 4).

Discussion

Distribution and characteristics of Greenland surge-type glaciers

Surge-type glaciers represent $\sim 1.2\%$ of all glaciers in Greenland, which is similar to estimates for the global population of surge-

type glaciers ($\sim 1\%$; Jiskoot and others, 2000; Sevestre and Benn, 2015). At individual cluster level, surge-type glaciers comprise 5.2% of all glaciers in the west cluster and 1.9% of all glaciers in the east cluster. These proportions are comparable to similar calculations (surge-type glaciers reported as a percentage of all glaciers) from other regional clusters, including the Canadian Arctic Archipelago (0.7%) (Copland and others, 2003); the Karakoram (1.9%), western Pamir (1.9%) and eastern Pamir (2.9%) (Guillet and others, 2022); the Russian High Arctic (4.6%) (Grant and others, 2009); and Iceland (4.7%) (Björnsson and others, 2003). All the above are markedly lower than estimates of the proportion of surge-type glaciers in the Svalbard cluster (e.g. Jiskoot and others, 2000; Bouchayer and others, 2022), where as high as 32.6% of all glaciers are suggested to be of surge-type (Farnsworth and others, 2016; Lovell and Boston, 2017).

Our inventory shows that the west and east surge clusters cover a larger geographical area than investigated in prior work. The west cluster was previously shown to be focused on Qeqertarsuaq and the Nuussuaq Peninsula (Weidick and others, 1992; Yde and Knudsen, 2007; Huber and others, 2020), but for the first time we have also identified surge-type glaciers on Svartenhuk Halvø at up to 72° N (Fig. 4). We also record more surge-type glaciers on the Nuussuaq Peninsula ($n = 22$; +17) than previously identified. The two main locations where surge-type glaciers are found in the east cluster are the Blossville Kyst/Geikie Plateau area (e.g. Weidick, 1988; Jiskoot and others, 2003) and the Scoresby Land/Stauning Alper area (Henriksen and Watt, 1968; Rutishauser, 1971; Woodward and others, 2002; Jiskoot and others, 2003) (Fig. 5). These two geographical areas form statistically significant sub-groups within the cluster based on P_a and T_a variables (Figs 8g and i; Table 4). The east cluster also extends further north (up to 73° N) than investigated in previous inventories (Weidick, 1988; Jiskoot and others, 2003).

A major difference between the west and east clusters is the size and configuration of surge-type glaciers. Surges in the west

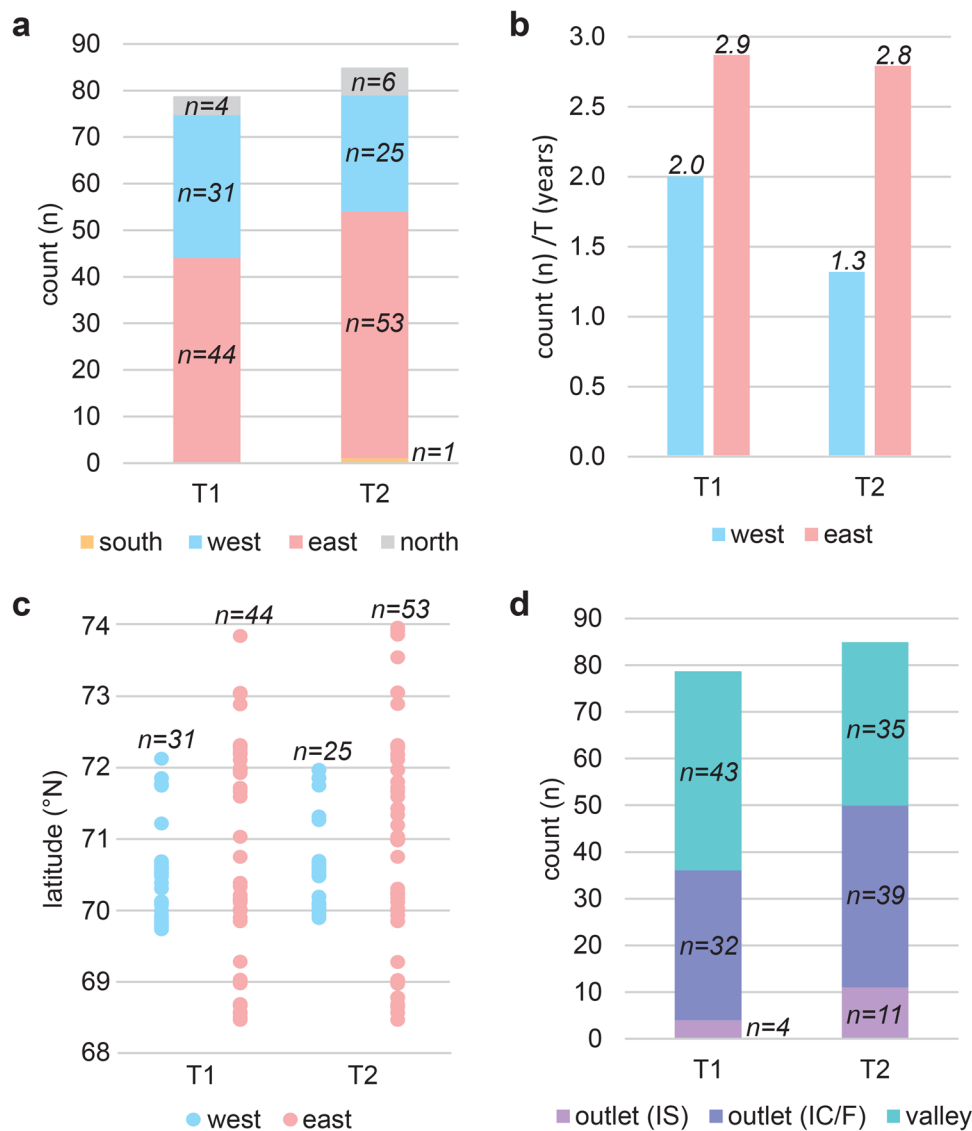


Figure 7. Temporal analysis of surge activity for glaciers with a surge index of 3 (observed surge-type glacier). We define surge activity here as evidence that a glacier experienced a surge active phase during the period of observation. Where surge-type glacier activity spans T1 (AeroDEM to GrIMP, ~1985–2000) and T2 (GrIMP to ArcticDEM, plus ASTER, ~2000–2019) the glacier has been counted in both (e.g. a glacier with surge activity observed in both 1999 and 2001 is counted in both T1 and T2). (a) Count of surge activity in T1 and T2 organised by cluster/region. (b) Surge activity in west and east clusters normalised by duration of T1 (15 years) and T2 (19 years). (c) Latitudinal range of surge activity in T1 and T2 for west and east clusters. (d) Count of surge activity in T1 and T2 organised by glacier type.

cluster tend to impact a large proportion of individual glaciers, with the downglacier propagation of the surge front resulting in the redistribution of significant volumes of ice to the glacier terminus (e.g. Fig. 3a). This expansion of the ablation area exposes a large percentage of the glacier's volume to post-surge melting, as observed at Kuannersuit Glacier, where it was estimated that 80–90% of the glacier's area was in the ablation area immediately following glacier termination in 1998 (Yde and Knudsen, 2007). By contrast, surges of tributaries and flow-units within large multi-branched glaciers in the east cluster do not always propagate the full length of the glacier system (e.g. Figs 3c and d) or into adjacent flow-units. Similar individual surge behaviour within complex glacier systems has been observed in Svalbard (e.g. Benn and others, 2009; Lovell and Fleming, 2022).

Beyond the west and east clusters, the large marine-terminating surge-type glaciers in the north are likely to be of particular interest in the future. Surges affect 38% of the 21 major outlet glaciers and drain 36% of the northern sector of the Greenland Ice Sheet (Hill

and others, 2017). While there is presently low ice discharge from this region (Mankoff and others, 2019; Mouginot and others, 2019), the surging behaviour of marine-terminating outlets across the Arctic region indicates the potential for rapid collapse (e.g. Jiskoot and others, 2012; McMillan and others, 2014; Willis and others, 2018; Nuth and others, 2019; Solgaard and others, 2020). In addition, increased iceberg production during marine-terminating glacier surges (e.g. Jiskoot and others, 2001; Truffer and others, 2021) presents a potential hazard for shipping (e.g. Bigg and others, 1996) offshore of the east cluster and in north and south Greenland (where all the marine-terminating surge-type glaciers are found), but not in the west cluster, where the surge-type glaciers all terminate on land.

Controls on surging

The enthalpy cycle model for surging asserts that climate exerts a first-order global control on the distribution of surge-type glaciers, and glacier geometry exerts a regional second-order control

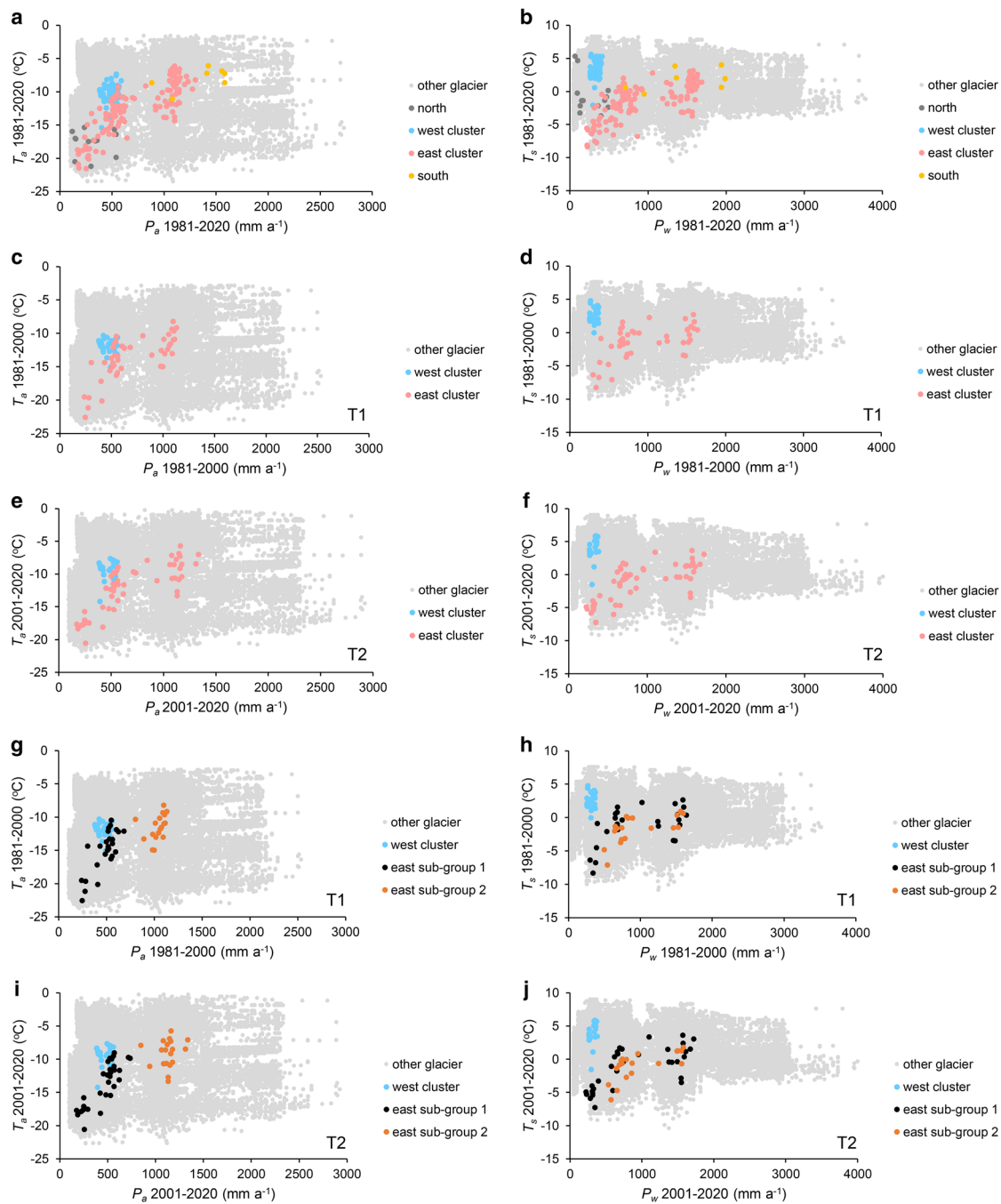


Figure 8. Climatic distribution of surge-type glaciers and nonsurge-type (other) glaciers. [Table 4](#) presents statistical analysis that compares the west and east cluster distributions plotted here. (a) Mean annual air temperature (T_a) against mean annual precipitation (P_a), 1981–2020 for all surge-type glaciers in our inventory (surge index of 1, 2 and 3). (b) Mean summer (JJA) air temperature (T_s) against mean winter (DJF) precipitation (P_w), 1981–2020 for all surge-type glaciers in our inventory (surge index of 1, 2 and 3). (c) T_a against P_a , 1981–2000 (T1) for all glaciers with a surge index of 3 in T1 in the west and east clusters. (d) T_s against P_w , 1981–2000 (T1) for all glaciers with a surge index of 3 in T1 in the west and east clusters. (e) T_a against P_a , 2001–2020 (T2) for all glaciers with a surge index of 3 in T2 in the west and east clusters. (f) T_s against P_w , 2001–2020 (T2) for all glaciers with a surge index of 3 in T2 in the west and east clusters. (g) T_a against P_a , 1981–2000 (T1) for all glaciers with a surge index of 3 in T1 in the west cluster and east cluster sub-groups 1 and 2. (h) T_s against P_w , 1981–2000 (T1) for all glaciers with a surge index of 3 in T1 in the west cluster and east cluster sub-groups 1 and 2. (i) T_a against P_a , 2001–2020 (T2) for all glaciers with a surge index of 3 in T2 in the west cluster and east cluster sub-groups 1 and 2. (j) T_s against P_w , 2001–2020 (T2) for all glaciers with a surge index of 3 in T2 in the west cluster and east cluster sub-groups 1 and 2. Temperature and precipitation data are from the monthly averaged ERA5-Land reanalysis dataset (Muñoz-Sabater, 2019). See text for references to east sub-groups 1 and 2 and [Figure 5](#) for their geographical coverage. See [Table 1](#) for surge index definition.

(Sevestre and Benn, 2015; Benn and others, 2019a). These suggestions hold true for Greenland, with the additional insight that climate variables can also be used to differentiate statistically significant geographical sub-groups of surge-type glaciers within regional groupings (i.e. separate groups and clusters within Greenland) and within clusters (i.e. sub-groups 1 and 2 within the east cluster) ([Fig. 8](#); [Table 4](#)). The climate thresholds for surging in Greenland can be broadly defined as -20 to -5°C T_a and

100 to 1250 mm P_a ([Fig. 8a](#)). Compared to the Sevestre and Benn (2015) climatic envelopes, the identified climate thresholds suggest most Greenland surge-type glaciers would plot in the overlap between their ‘Arctic Ring’ and Canadian High Arctic clusters. Our T_s ranges for Greenland ([Fig. 8b](#)) are towards the cooler end of the ‘Arctic Ring’ envelope as shown in Sevestre and Benn (2015), which probably reflects our inclusion of additional surge-type glaciers in northern Greenland and the northern

Table 4. Statistical analysis (Mann–Whitney U tests) comparing the climatic distribution of surge-type glaciers in the west and east clusters.

Compared groups	n	ERA5-Land climate variables			
		P_a (mm a ⁻¹)	T_a (°C)	P_w (mm a ⁻¹)	T_s (°C)
W cluster and E cluster, 1981–2020	255	$U = 5075, p < 0.001$	$U = 11\ 352, p < 0.001$	$U = 1529, p = 0.000$	$U = 15\ 849, p = 0.000$
W cluster and E cluster, T1 (1981–2000)	75*	$U = 285, p < 0.001$	$U = 920, p = 0.010$	$U = 25, p < 0.001$	$U = 1298, p < 0.001$
W cluster and E cluster, T2 (2001–2020)	78*	$U = 372, p = 0.002$	$U = 975, p < 0.001$	$U = 143, p < 0.001$	$U = 1262, p < 0.001$
W cluster T1 (1981–2000) and W cluster T2 (2001–2020)	56*	$U = 414, p = 0.662$	$U = 732, p < 0.001$	$U = 460, p = 0.232$	$U = 618, p < 0.001$
E cluster T1 (1981–2000) and E cluster T2 (2001–2020)	97*	$U = 1180, p = 0.919$	$U = 1479, p = 0.023$	$U = 1108, p = 0.674$	$U = 1265, p = 0.473$
E cluster sub-group 1 and E cluster sub-group 2, 1981–2020	132	$U = 4275, p = 0.000$	$U = 3904, p < 0.001$	$U = 4275, p = 0.000$	$U = 4275, p = 0.000$
E cluster sub-group 1 and E cluster sub-group 2, T1 (1981–2000)	44*	$U = 468, p < 0.001$	$U = 394, p < 0.001$	$U = 248, p = 0.738$	$U = 185, p = 0.242$
E cluster sub-group 1 and E cluster sub-group 2, T2 (2001–2020)	53*	$U = 646, p < 0.001$	$U = 570, p < 0.001$	$U = 368, p = 0.404$	$U = 322, p = 0.985$
E cluster sub-group 1 and W cluster, T1 (1981–2000)	57*	$U = 285, p = 0.059$	$U = 683, p < 0.001$	$U = 25, p < 0.001$	$U = 744, p < 0.001$
E cluster sub-group 1 and W cluster, T2 (2001–2020)	59*	$U = 372, p = 0.416$	$U = 776, p < 0.001$	$U = 143, p < 0.001$	$U = 805, p < 0.001$

Values in bold indicate there is a statistically significant difference ($p < 0.05$) in climate conditions between groups. U = Mann–Whitney U test statistic; P_a = mean annual precipitation; T_a = mean annual air temperature; P_w = mean winter precipitation; T_s = mean summer air temperature. n = all surge-type glaciers, n^* = surge-type glaciers with a surge index of 3 (observed surge-type glacier). See Table 1 for surge index definition and Figure 8 for plots of the climatic distribution.

parts of the west and east clusters that were not in the Sevestre and Benn (2015) dataset. In particular, the cooler, drier climate of the northern surge-type glaciers, west cluster and east cluster sub-group 1 (glaciers mostly located to the north of Scoresby Sund; Fig. 5) shares similarities with the Canadian High Arctic climatic envelope, whereas the warmer, wetter east cluster sub-group 2 (Blosseville Kyst/Geikie Plateau glaciers; Fig. 5) and southern surge-type glaciers fit better within the Sevestre and Benn (2015) ‘Arctic Ring’ envelope.

The geometric attributes of surge-type glaciers provide evidence for the second-order control on surging. Surge-type glaciers in both the west and east clusters are larger, longer, cover a greater elevation range and generally have shallower slopes than other glaciers (Fig. 6). These characteristics agree with similar data from the global database of surge-type glaciers (Sevestre and Benn, 2015) and that reported from the surge clusters in Alaska (Clarke, 1991), east Greenland (Jiskoot and others, 2003), Iceland (Björnsson and others, 2003), Svalbard (Jiskoot and others, 1998), the Russian High Arctic (Grant and others, 2009) and High Mountain Asia (Guillet and others, 2022).

We have not explored the role of underlying geology in controlling surge-type glacier distribution (e.g. Post, 1969; Crompton and Flowers, 2016). It has been noted in previous work that both the west and east Greenland surge-type glacier clusters are in basalt-dominated regions (Weidick, 1988; Weidick and others, 1992), although no clear relationship between bedrock lithology and surge-type glaciers was identified by Jiskoot and others (2003) in the east cluster. However, Jiskoot and others (2003) did find that glaciers overlying bedrock that was younger than Precambrian in age had increased surge potential in east Greenland. The relationship between surging and bedrock lithology appears to be particularly strong in the Svalbard cluster, where it has been established that surge-type glaciers tend to be underlain by fine-grained sedimentary lithologies (Hamilton and Dowdeswell, 1996; Jiskoot and others, 1998, 2000).

Changing surge behaviour over time

Our temporal analysis of surge activity appears to suggest that fewer glaciers were surging in T2 compared to T1 in the west cluster, indicating that there has been a reduction in surge activity between the time periods (Fig. 7b). We suggest that this apparent reduction in surging could be controlled by glacier thinning as the climate warms in the region. Western Greenland has experienced very strong warming since the 1980s (Hanna and others, 2012, 2021; Abermann and others, 2017) and the glaciers in the west cluster are estimated to have experienced an annual mass change of -1.7 ± 0.6 Gt yr⁻¹ over approximately this same period (Huber and others, 2020). Our climate analysis demonstrates that surge-

type glaciers in the west cluster experienced statistically significant warming of $\sim 1^\circ\text{C}$ for both T_a and T_s between T1 and T2 (Table 4). The impact of such warming on glacier mass balance can be enhanced for surge-type glaciers, which have been shown to undergo greater recession than other (nonsurge-type) glaciers in the immediate post-surge quiescent phase, typically because of the large mass redistribution to lower elevations associated with the surge active phase (Yde and Knudsen, 2007; Bhattacharya and others, 2021; Guillet and others, 2022). We suggest that the post-surge thinning effect is especially strong in the west cluster, where most glaciers have been receding and losing mass in recent decades (Yde and Knudsen, 2007; Leclercq and others, 2012; Huber and others, 2020). Surge-type glaciers here are typically small valley glaciers or icefield outlet glaciers with simple configurations (i.e. single trunk glaciers). When surges occur, they impact most of the glacier, resulting in a large proportion of the overall glacier mass being transferred to the ablation area. This likely accounts for the long surge return periods in the west cluster (Yde and Knudsen, 2007), as the post-surge recovery takes longer. Our data also suggests that across all surge-type glaciers in Greenland, fewer valley glaciers surged in T2 compared to outlet glaciers (Fig. 7d). This is consistent with the impact of surges, post-surge thinning and overall negative mass balance being greater on valley glaciers (generally smaller and simple configurations) than on larger multi-branched outlet glaciers.

For surge-type glaciers to continue the surge cycle following surge termination, they have to build-up sufficient mass in the accumulation area during the quiescent phase. This becomes difficult if the regional mass balance conditions are strongly negative (e.g. Małeckı and others, 2013). Glacier thinning can also result in a switch in glacier thermal regime from polythermal to a largely cold-based, inactive state (e.g. Sevestre and others, 2015; Carrivick and others, 2023b). Cold air waves in winter can penetrate to the bed of thinner glaciers more easily, reducing pressure melting and the production of basal meltwater (Björnsson and others, 1996; Lovell and others, 2015), and thus limiting basal sliding. In a region where surge-type glaciers are likely to be polythermal (e.g. Roberts and others, 2009), a switch to a cold-based thermal regime may mean that some surge-type glaciers in the west cluster will be unable to surge under present climate conditions, as has been observed in Svalbard (Hansen, 2003; Małeckı and others, 2013; Lovell and others, 2015; Sevestre and others, 2015; Benn and others, 2019a).

The suggestion that a warmer climate is struggling to support surges of the typically small, land-terminating glaciers in the west cluster is consistent with the growing body of evidence on the importance of mass balance, and thus ultimately climate, in controlling glacier surges (e.g. Dowdeswell and others, 1995; Eisen and others, 2001; Flowers and others, 2011; Bevington and Copland,

2014; Sevestre and Benn, 2015; Kochtitzky and others, 2020). If climatic envelopes conducive to surging shift away from previously optimal conditions in recognised surge clusters, we might expect some surge-type glaciers to be removed from the surge cycle entirely (e.g. Hansen, 2003; Malecki and others, 2013).

Summary and conclusions

We present the first systematic inventory of surge-type glaciers in Greenland, compiled from previous studies and the analysis of multitemporal satellite images and difference digital elevation models (dDEMs). We identify 274 surge-type glaciers, representing an increase of 37% compared to previous work. The majority of the 74 newly identified surge-type glaciers are found in the west and east clusters, extending both clusters approximately one degree of latitude further north into areas that were unexplored in previous inventories. Surge-type glaciers are larger in the east cluster than the west cluster, despite overall glacier size distributions being similar in both regions. Surges tend to impact the whole glacier trunk in the west, whereas individual tributaries or flow-units of large multi-branched glaciers in the east can show individual surge behaviour.

Analysis of ERA5-Land climate data show that surge-type glaciers in the different geographical groups occur in well-defined and statistically significant climatic envelopes. The east cluster resolves into two sub-groups with statistically distinct climate conditions: the group of surge-type glaciers mostly located to the north of Scoresby Sund (cooler and drier) and the Blossville Kyst/Geikie Plateau group (warmer and wetter). We provide the first analysis of spatio-temporal patterns of surging in Greenland by summarising surge activity (defined as the number of glaciers observed to be in the surge active phase) during the time periods T1 (~1985 to 2000) and T2 (~2000 to 2019). Overall surge activity was similar in both T1 and T2, but there appears to be a reduction in surge activity in the west cluster in T2. This is coincident with statistically significant warming of ~1°C in the cluster between the two time periods. Reduced surge activity in the west cluster could potentially indicate the start of a process whereby the climate is shifting away from the optimal climatic envelope for surging in the region, with the possible outcome that the west cluster will continue to experience less surging over time.

Future work on surges and climate should focus on: ongoing updates of regional and global surge-type glacier inventories, which could be achieved using emerging automated methods for detecting surge behaviour (e.g. Herreid and Truffer, 2016; Leclercq and others, 2021; Kääb and others, 2023; Li and others, 2023); further exploration of spatial and temporal trends in regional surge behaviour and their relationship to climate; and a better understanding of the underlying processes that control the spectrum of glacier dynamics that encompasses surging.

Supplementary material. The supplementary material for this article can be found at <https://doi.org/10.1017/jog.2023.61>.

Data. GIS files of the Greenland surge-type glacier inventory are available at <https://doi.org/10.17029/ca8a3d97-536a-4f09-9c86-895ed54f6918>.

Acknowledgements. Paul Carter is thanked for his help formatting GIS files of previous surge-type glacier inventories. We thank two anonymous reviewers and the Scientific Editor, Hester Jiskoot, for their helpful comments for improving the work presented here.

References

- Abermann J and 5 others** (2017) Hotspots and key periods of Greenland climate change during the past six decades. *Ambio* **46**(1), 3–11. doi: [10.1007/s13280-016-0861-y](https://doi.org/10.1007/s13280-016-0861-y)

- Benn DI and 5 others** (2019b) Mass and enthalpy budget evolution during the surge of a polythermal glacier: a test of theory. *Journal of Glaciology* **65** (253), 717–731. doi: [10.1017/jog.2019.63](https://doi.org/10.1017/jog.2019.63)
- Benn DI, Fowler AC, Hewitt I and Sevestre H** (2019a) A general theory of glacier surges. *Journal of Glaciology* **65**(253), 701–716. doi: [10.1017/jog.2019.62](https://doi.org/10.1017/jog.2019.62)
- Benn DI, Hewitt I and Luckman A** (2023) Enthalpy balance theory unifies diverse glacier surge behaviour. *Annals of Glaciology*. doi: [10.1017/aog.2023.23](https://doi.org/10.1017/aog.2023.23)
- Benn DI, Kristensen L and Gulley JD** (2009) Surge propagation constrained by a persistent subglacial conduit, Bakaninbreen–Paulabreen, Svalbard. *Annals of Glaciology* **50**(52), 81–86. doi: [10.3189/172756409789624337](https://doi.org/10.3189/172756409789624337)
- Berdahl M and 9 others** (2018) Southeast Greenland winter precipitation strongly linked to the Icelandic low position. *Journal of Climate* **31**(11), 4483–4500. doi: [10.1175/JCLI-D-17-0622.1](https://doi.org/10.1175/JCLI-D-17-0622.1)
- Bevington A and Copland L** (2014) Characteristics of the last five surges of Lowell Glacier, Yukon, Canada, since 1948. *Journal of Glaciology* **60**(219), 113–123. doi: [10.3189/2014JoG13J134](https://doi.org/10.3189/2014JoG13J134)
- Bhambri R, Hewitt K, Kawishwar P and Pratap B** (2017) Surge-type and surge-modified glaciers in the Karakoram. *Scientific Reports* **7**(1), 1–14. doi: [10.1038/s41598-017-15473-8](https://doi.org/10.1038/s41598-017-15473-8)
- Bhattacharya A and 8 others** (2021) High Mountain Asian glacier response to climate revealed by multi-temporal satellite observations since the 1960s. *Nature Communications* **12**(1), 1–13. doi: [10.1038/s41467-021-24180](https://doi.org/10.1038/s41467-021-24180)
- Bigg GR, Wadley MR, Stevens DP and Johnson JA** (1996) Prediction of ice-berg trajectories for the North Atlantic and Arctic Oceans. *Geophysical Research Letters* **23**(24), 3587–3590. doi: [10.1029/96GL03369](https://doi.org/10.1029/96GL03369)
- Bjork AA, Kruse LM and Michaelsen PB** (2015) Brief communication: getting Greenland's glaciers right—a new data set of all official Greenlandic glacier names. *The Cryosphere* **9**(6), 2215–2218. doi: [10.5194/tc-9-2215-2015](https://doi.org/10.5194/tc-9-2215-2015)
- Björnsson H and 6 others** (1996) The thermal regime of sub-polar glaciers mapped by multi-frequency radio-echo sounding. *Journal of Glaciology* **42**(140), 23–32. doi: [10.3189/S0022143000030495](https://doi.org/10.3189/S0022143000030495)
- Björnsson H, Pálsson F, Sigurdsson O and Flowers GE** (2003) Surges of glaciers in Iceland. *Annals of Glaciology* **36**, 82–90. doi: [10.3189/172756403781816365](https://doi.org/10.3189/172756403781816365)
- Bolch T and 6 others** (2013) Mass loss of Greenland's glaciers and ice caps 2003–2008 revealed from ICESat laser altimetry data. *Geophysical Research Letters* **40**(5), 875–881. doi: [10.1002/grl.50270](https://doi.org/10.1002/grl.50270)
- Bouchayer C, Aiken JM, Thøgersen K, Renard F and Schuler TV** (2022) A machine learning framework to automate the classification of surge-type glaciers in Svalbard. *Journal of Geophysical Research: Earth Surface* **127** (7), e2022JF006597. doi: [10.1029/2022JF006597](https://doi.org/10.1029/2022JF006597)
- Brough S, Carr JR, Ross N and Lea JM** (2023) Ocean-forcing and glacier-specific factors drive differing glacier response across the 69 °N boundary, east Greenland. *Journal of Geophysical Research: Earth Surface* **128**, e2022JF006857. doi: [10.1029/2022JF006857](https://doi.org/10.1029/2022JF006857)
- Carrivick JL and 6 others** (2019) Accelerated volume loss in glacier ablation zones of NE Greenland, little ice age to present. *Geophysical Research Letters* **46**(3), 1476–1484. doi: [10.1029/2018GL081383](https://doi.org/10.1029/2018GL081383)
- Carrivick JL and 11 others** (2023a) Mass loss of glaciers and ice caps across Greenland since the little ice age. *Geophysical Research Letters* **50**, e2023GL103950. doi: [10.1029/2023GL103950](https://doi.org/10.1029/2023GL103950)
- Carrivick JL, Smith MW, Sutherland JL and Grimes M** (2023b) Cooling glaciers in a warming climate since the little ice age at Qaanaaq, northwest Kalaallit Nunaat (Greenland). *Earth Surface Processes and Landforms*, 1–17. doi: [10.1002/esp.5638](https://doi.org/10.1002/esp.5638)
- Carrivick JL, Tweed F, James WM and Jóhannesson T** (2017) Surface and geometry changes during the first documented surge of Kverkjökull, central Iceland. *Jökull* **66**, 27–49. doi: [10.33799/jokull2016.66.027](https://doi.org/10.33799/jokull2016.66.027)
- Citterio M, Paul F, Ahlström AP, Jepsen HF and Weidick A** (2009) Remote sensing of glacier change in west Greenland: accounting for the occurrence of surge-type glaciers. *Annals of Glaciology* **50**(53), 70–80. doi: [10.3189/172756410790595813](https://doi.org/10.3189/172756410790595813)
- Clarke GK** (1991) Length, width and slope influences on glacier surging. *Journal of Glaciology* **37**(126), 236–246. doi: [10.3189/S0022143000007255](https://doi.org/10.3189/S0022143000007255)
- Clarke GK, Schmok JP, Ommanney CSL and Collins SG** (1986) Characteristics of surge-type glaciers. *Journal of Geophysical Research: Solid Earth* **91**(B7), 7165–7180. doi: [10.1029/JB091iB07p07165](https://doi.org/10.1029/JB091iB07p07165)
- Colvill AJ** (1984) Some observations on glacier surges with notes on the Roslin glacier, east Greenland. In Miller KJ ed. *The International Karakoram*

- Project. Proceedings of the International Conference*, vol. 1, Cambridge: Cambridge University Press, pp. 64–75.
- Copland L, Sharp MJ and Dowdeswell JA** (2003) The distribution and flow characteristics of surge-type glaciers in the Canadian High Arctic. *Annals of Glaciology* **36**, 73–81. doi: [10.3189/172756403781816301](https://doi.org/10.3189/172756403781816301)
- Crompton JW and Flowers GE** (2016) Correlations of suspended sediment size with bedrock lithology and glacier dynamics. *Annals of Glaciology* **57** (72), 142–150. doi: [10.1017/aog.2016.6](https://doi.org/10.1017/aog.2016.6)
- Dowdeswell JA, Hodgkins R, Nuttall AM, Hagen JO and Hamilton GS** (1995) Mass balance change as a control on the frequency and occurrence of glacier surges in Svalbard, Norwegian High Arctic. *Geophysical Research Letters* **22**(21), 2909–2912. doi: [10.1029/95GL02821](https://doi.org/10.1029/95GL02821)
- Dunse T and 5 others** (2015) Glacier-surge mechanisms promoted by a hydro-thermodynamic feedback to summer melt. *The Cryosphere* **9**(1), 197–215. doi: [10.5194/tc-9-197-2015](https://doi.org/10.5194/tc-9-197-2015)
- Eisen O, Harrison WD and Raymond CF** (2001) The surges of Variegated Glacier, Alaska, USA, and their connection to climate and mass balance. *Journal of Glaciology* **47**(158), 351–358. doi: [10.3189/172756501781832179](https://doi.org/10.3189/172756501781832179)
- Falaschi D and 5 others** (2018) New evidence of glacier surges in the central Andes of Argentina and Chile. *Progress in Physical Geography: Earth and Environment* **42**(6), 792–825. doi: [10.1177/0309133318803014](https://doi.org/10.1177/0309133318803014)
- Farnsworth WR, Ingólfsson Ó, Retelle M and Schomacker A** (2016) Over 400 previously undocumented Svalbard surge-type glaciers identified. *Geomorphology* **264**, 52–60. doi: [10.1016/j.geomorph.2016.03.025](https://doi.org/10.1016/j.geomorph.2016.03.025)
- Finger Higgs RA and 5 others** (2019) Changing lake dynamics indicate a drier Arctic in western Greenland. *Journal of Geophysical Research: Biogeosciences* **124**(4), 870–883. doi: [10.1029/2018JG004879](https://doi.org/10.1029/2018JG004879)
- Flowers GE, Roux N, Pimentel S and Schoof CG** (2011) Present dynamics and future prognosis of a slowly surging glacier. *The Cryosphere* **5**(1), 299–313. doi: [10.5194/tc-5-299-2011](https://doi.org/10.5194/tc-5-299-2011)
- Fowler AC, Murray T and Ng FSL** (2001) Thermally controlled glacier surging. *Journal of Glaciology* **47**(159), 527–538. doi: [10.3189/172756501781831792](https://doi.org/10.3189/172756501781831792)
- Friese-Greene TW and Pert GJ** (1965) Velocity fluctuations of the Bersaekerbrae, east Greenland. *Journal of Glaciology* **5**(41), 739–747.
- Gardner AS and 15 others** (2013) A reconciled estimate of glacier contributions to sea level rise: 2003 to 2009. *Science* **340**(6134), 852–857. doi: [10.1126/science.1234532](https://doi.org/10.1126/science.1234532)
- Gilbert R, Nielsen N, Möller H, Desloges JR and Rasch M** (2002) Glacimarine sedimentation in Kangerdluk (Disko Fjord), west Greenland, in response to a surging glacier. *Marine Geology* **191**(1–2), 1–18. doi: [10.1016/S0025-3227\(02\)00543-1](https://doi.org/10.1016/S0025-3227(02)00543-1)
- Goerlich F, Bolch T and Paul F** (2020) More dynamic than expected: an updated survey of surging glaciers in the Pamir. *Earth System Science Data* **12**(4), 3161–3176. doi: [10.5194/essd-12-3161-2020](https://doi.org/10.5194/essd-12-3161-2020)
- Grant KL, Stokes CR and Evans IS** (2009) Identification and characteristics of surge-type glaciers on Novaya Zemlya, Russian Arctic. *Journal of Glaciology* **55**(194), 960–972. doi: [10.3189/002214309790794940](https://doi.org/10.3189/002214309790794940)
- Guillet G and 6 others** (2022) A regionally resolved inventory of High Mountain Asia surge-type glaciers, derived from a multi-factor remote sensing approach. *The Cryosphere* **16**, 603–623. doi: [10.5194/tc-16-603-2022](https://doi.org/10.5194/tc-16-603-2022)
- Haga ON and 5 others** (2020) From high friction zone to frontal collapse: dynamics of an ongoing tidewater glacier surge, Negribreen, Svalbard. *Journal of Glaciology* **66**(259), 742–754. doi: [10.1017/jog.2020.43](https://doi.org/10.1017/jog.2020.43)
- Hamilton GS and Dowdeswell JA** (1996) Controls on glacier surging in Svalbard. *Journal of Glaciology* **42**(140), 157–168. doi: [10.3189/S0022143000030616](https://doi.org/10.3189/S0022143000030616)
- Hanna E and 8 others** (2021) Greenland surface air temperature changes from 1981 to 2019 and implications for ice-sheet melt and mass-balance change. *International Journal of Climatology* **41**, E1336–E1352. doi: [10.1002/joc.6771](https://doi.org/10.1002/joc.6771)
- Hanna E, Mernild SH, Cappelen J and Steffen K** (2012) Recent warming in Greenland in a long-term instrumental (1881–2012) climatic context: I. Evaluation of surface air temperature records. *Environmental Research Letters* **7**(4), 045404. doi: [10.1088/1748-9326/7/4/045404](https://doi.org/10.1088/1748-9326/7/4/045404)
- Hansen S** (2003) From surge-type to non-surge-type glacier behaviour: Midre Lovénbreen, Svalbard. *Annals of Glaciology* **36**, 97–102. doi: [10.3189/172756403781816383](https://doi.org/10.3189/172756403781816383)
- Harrison WD and Post AS** (2003) How much do we really know about glacier surging? *Annals of Glaciology* **36**, 1–6. doi: [10.3189/172756403781816185](https://doi.org/10.3189/172756403781816185)
- Henriksen N and Watt WS** (1968) Geological reconnaissance of the Scoresby Sund fjord complex. *Rapport Grønlands Geologiske Undersøgelse* **15**, 72–77. doi: [10.34194/rapgu.v15.7181](https://doi.org/10.34194/rapgu.v15.7181)
- Herreid S and Truffer M** (2016) Automated detection of unstable glacier flow and a spectrum of speedup behavior in the Alaska Range. *Journal of Geophysical Research: Earth Surface* **121**(1), 64–81. doi: [10.1002/2015JF003502](https://doi.org/10.1002/2015JF003502)
- Hersbach and 42 others** (2020) The ERA5 global reanalysis. *Quarterly Journal of the Royal Meteorological Society* **146**(730), 1999–2049. doi: [10.1002/qj.3803](https://doi.org/10.1002/qj.3803)
- Hewitt K** (1969) Glacier surges in the Karakoram Himalaya (central Asia). *Canadian Journal of Earth Sciences* **6**(4), 1009–1018. doi: [10.1139/e69-106](https://doi.org/10.1139/e69-106)
- Higgins AK** (1991) North Greenland glacier velocities and calf ice production. *Polarforschung* **60**(1), 1–23.
- Hill EA, Carr JR and Stokes CR** (2017) A review of recent changes in major marine-terminating outlet glaciers in northern Greenland. *Frontiers in Earth Science* **4**, 111. doi: [10.3389/feart.2016.00111](https://doi.org/10.3389/feart.2016.00111)
- Howat IM, Negrete A and Smith BE** (2014) The Greenland ice mapping project (GIMP) land classification and surface elevation data sets. *The Cryosphere* **8**(4), 1509–1518. doi: [10.5194/tc-8-1509-2014](https://doi.org/10.5194/tc-8-1509-2014)
- Huber J, McNabb R and Zemp M** (2020) Elevation changes of west-central Greenland glaciers from 1985 to 2012 from remote sensing. *Frontiers in Earth Science* **8**, 35. doi: [10.3389/feart.2020.00035](https://doi.org/10.3389/feart.2020.00035)
- Hugonnet R and 10 others** (2021) Accelerated global glacier mass loss in the early twenty-first century. *Nature* **592**(7856), 726–731. doi: [10.1038/s41586-021-03436-z](https://doi.org/10.1038/s41586-021-03436-z)
- Jiskoot H** (2002) *Central East Greenland GLIMS Glacier Database*. Boulder, CO: National Snow and Ice Data Center/World Data Center for Glaciology. doi: [10.7265/N5V98602](https://doi.org/10.7265/N5V98602)
- Jiskoot H, Boyle P and Murray T** (1998) The incidence of glacier surging in Svalbard: evidence from multivariate statistics. *Computers & Geosciences* **24** (4), 387–399. doi: [10.1016/S0098-3004\(98\)00033-8](https://doi.org/10.1016/S0098-3004(98)00033-8)
- Jiskoot H and Juhlin DT** (2009) Surge of a small east Greenland glacier, 2001–2007, suggests Svalbard-type surge mechanism. *Journal of Glaciology* **55**(191), 567–570. doi: [10.3189/002214309788816605](https://doi.org/10.3189/002214309788816605)
- Jiskoot H, Juhlin D, St Pierre H and Citterio M** (2012) Tidewater glacier fluctuations in central east Greenland coastal and fjord regions (1980s–2005). *Annals of Glaciology* **53**(60), 35–44. doi: [10.3189/2012AoG60A030](https://doi.org/10.3189/2012AoG60A030)
- Jiskoot H, Murray T and Boyle P** (2000) Controls on the distribution of surge-type glaciers in Svalbard. *Journal of Glaciology* **46**(154), 412–422. doi: [10.3189/172756500781833115](https://doi.org/10.3189/172756500781833115)
- Jiskoot H, Murray T and Luckman A** (2003) Surge potential and drainage-basin characteristics in east Greenland. *Annals of Glaciology* **36**, 142–148. doi: [10.3189/172756403781816220](https://doi.org/10.3189/172756403781816220)
- Jiskoot H, Pedersen AK and Murray T** (2001) Multi-model photogrammetric analysis of the 1990s surge of Sortebræ, east Greenland. *Journal of Glaciology* **47**(159), 677–687. doi: [10.3189/172756501781831846](https://doi.org/10.3189/172756501781831846)
- Joughin I, Tulaczyk S, Fahnestock M and Kwok R** (1996) A mini-surge on the Ryder Glacier, Greenland, observed by satellite radar interferometry. *Science* **274**(5285), 228–230. doi: [10.1126/science.274.5285.228](https://doi.org/10.1126/science.274.5285.228)
- Kääb A and 14 others** (2021) Sudden large-volume detachments of low-angle mountain glaciers—more frequent than thought? *The Cryosphere* **15**(4), 1751–1785. doi: [10.5194/tc-15-1751-2021](https://doi.org/10.5194/tc-15-1751-2021)
- Kääb A, Bazilova V, Leclercq PW, Mannerfelt ES and Strozzini T** (2023) Global clustering of recent glacier surges from radar backscatter data, 2017–2022. *Journal of Glaciology*, 1–9. doi: [10.1017/jog.2023.35](https://doi.org/10.1017/jog.2023.35)
- Kamb B and 7 others** (1985) Glacier surge mechanism: 1982–1983 surge of Variegated Glacier, Alaska. *Science* **227**(4686), 469–479. doi: [10.1126/science.227.4686.469](https://doi.org/10.1126/science.227.4686.469)
- Khan SA and 8 others** (2022) Accelerating ice loss from peripheral glaciers in north Greenland. *Geophysical Research Letters* **49**, e2022GL098915. doi: [10.1029/2022GL098915](https://doi.org/10.1029/2022GL098915)
- King O, Bhattacharya A and Bolch T** (2021) The presence and influence of glacier surging around the Geladandong ice caps, north east Tibetan Plateau. *Advances in Climate Change Research* **12**(3), 299–312. doi: [10.1016/j.accre.2021.05.001](https://doi.org/10.1016/j.accre.2021.05.001)
- Koch JP and Wegener A** (1930) *Wissenschaftliche Ergebnisse der dänischen Expedition nach Dronning Louises Land und quer über das Inlandeis von Nordgrönland 1912–1913 unter Leitung von Hauptmann J. P. Koch*. *Meddr Grønland* **75**(1), 676.
- Kochitzky W and 9 others** (2020) Climate and surging of Donjek glacier, Yukon, Canada. *Arctic, Antarctic, and Alpine Research* **52**(1), 264–280. doi: [10.1080/15230430.2020.1744397](https://doi.org/10.1080/15230430.2020.1744397)
- Korsgaard NJ and 6 others** (2016) Digital elevation model and orthophotographs of Greenland based on aerial photographs from 1978–1987. *Scientific Data* **3**(1), 1–5. doi: [10.1038/sdata.2016.32](https://doi.org/10.1038/sdata.2016.32)

- Krieger L, Floricioiu D and Neckel N** (2020) Drainage basin delineation for outlet glaciers of northeast Greenland based on Sentinel-1 ice velocities and TanDEM-X elevations. *Remote Sensing of Environment* **237**, 111483. doi: [10.1016/j.rse.2019.111483](https://doi.org/10.1016/j.rse.2019.111483)
- Lauzon B and 5 others** (2023) Dynamics throughout a complete surge of Iceberg Glacier on western Axel Heiberg Island, Canadian High Arctic. *Journal of Glaciology* **12**, 1–8. doi: [10.1017/jog.2023.20](https://doi.org/10.1017/jog.2023.20)
- Leclercq PW and 5 others** (2012) Brief communication: historical glacier length changes in west Greenland. *The Cryosphere* **6**(6), 1339–1343. doi: [10.5194/tc-6-1339-2012](https://doi.org/10.5194/tc-6-1339-2012)
- Leclercq PW, Kääh A and Altena B** (2021) Brief communication: detection of glacier surge activity using cloud computing of Sentinel-1 radar data. *The Cryosphere* **15**(10), 4901–4907. doi: [10.5194/tc-15-4901-2021](https://doi.org/10.5194/tc-15-4901-2021)
- Lewis G and 9 others** (2019) Recent precipitation decrease across the western Greenland ice sheet percolation zone. *The Cryosphere* **13**(11), 2797–2815. doi: [10.5194/tc-13-2797-2019](https://doi.org/10.5194/tc-13-2797-2019)
- Li G and 7 others** (2023) Characterizing the surge behaviour and associated ice-dammed lake evolution of the Kyagar Glacier in the Karakoram. *The Cryosphere Discussions* **13**, 1–26. doi: [10.5194/tc-2022-253](https://doi.org/10.5194/tc-2022-253)
- Liboutry L** (1998) Glaciers of the Dry Andes. In Williams RS and Ferrigno JG eds. *Satellite Image Atlas of Glaciers of the World South America*. USGS Professional Paper 1386-I-6, pp. 119–137. doi: <https://pubs.usgs.gov/pp/p1386i/index.html>
- Lovell H and 5 others** (2015) Former dynamic behaviour of a cold-based valley glacier on Svalbard revealed by basal ice and structural glaciology investigations. *Journal of Glaciology* **61**(226), 309–328. doi: [10.3189/2015jog14j120](https://doi.org/10.3189/2015jog14j120)
- Lovell H and Boston CM** (2017) Glacitectonic composite ridge systems and surge-type glaciers: an updated correlation based on Svalbard, Norway. *arktos* **3**(1), 2. doi: [10.1007/s41063-017-0028-5](https://doi.org/10.1007/s41063-017-0028-5)
- Lovell AM, Carr JR and Stokes CR** (2018) Topographic controls on the surging behaviour of Sabche Glacier, Nepal (1967 to 2017). *Remote Sensing of Environment* **210**, 434–443. doi: [10.1016/j.rse.2018.03.036](https://doi.org/10.1016/j.rse.2018.03.036)
- Lovell H and Fleming EJ** (2022) Structural evolution during a surge in the Paulabreen glacier system, Svalbard. *Journal of Glaciology* **69**(273), 141–152. doi: [10.1017/jog.2022.53](https://doi.org/10.1017/jog.2022.53)
- Lv M and 7 others** (2019) Characterizing the behaviour of surge- and non-surge-type glaciers in the Kingata Mountains, eastern Pamir, from 1999 to 2016. *The Cryosphere* **13**(1), 219–236. doi: [10.5194/tc-13-219-2019](https://doi.org/10.5194/tc-13-219-2019)
- Malecki J, Faucherre S and Strzelecki M** (2013) Post- surge geometry and thermal structure of Horbyebreen, central Spitsbergen. *Polish Polar Research* **34**(3), 305–321. doi: [10.2478/popore-2013-0019](https://doi.org/10.2478/popore-2013-0019)
- Mankoff KD and 10 others** (2019) Greenland ice sheet solid ice discharge from 1986 through 2017. *Earth System Science Data* **11**(2), 769–786. doi: [10.5194/essd-11-769-2019](https://doi.org/10.5194/essd-11-769-2019)
- McMillan M and 14 others** (2014) Rapid dynamic activation of a marine-based Arctic ice cap. *Geophysical Research Letters* **41**(24), 8902–8909. doi: [10.1002/2014GL062255](https://doi.org/10.1002/2014GL062255)
- Meier MF and Post A** (1969) What are glacier surges? *Canadian Journal of Earth Sciences* **6**(4), 807–817. doi: [10.1139/e69-081](https://doi.org/10.1139/e69-081)
- Melvold K and Hagen JO** (1998) Evolution of a surge-type glacier in its quiescent phase: Kongsvegen, Spitsbergen, 1964–95. *Journal of Glaciology* **44** (147), 394–404. doi: [10.3189/S0022143000002720](https://doi.org/10.3189/S0022143000002720)
- Mernild SH and 6 others** (2011) Increasing mass loss from Greenland's Mittivakkat Gletscher. *The Cryosphere* **5**(2), 341–348. doi: [10.5194/tc-5-341-2011](https://doi.org/10.5194/tc-5-341-2011)
- Mernild SH and 8 others** (2015) Greenland precipitation trends in a long-term instrumental climate context (1890–2012): evaluation of coastal and ice core records. *International Journal of Climatology* **35**(2), 303–320. doi: doi.org/10.1002/joc.3986
- Mernild SH, Hanna E, Yde JC, Cappelen J and Malmros JK** (2014) Coastal Greenland air temperature extremes and trends 1890–2010: annual and monthly analysis. *International Journal of Climatology* **34**(5), 1472–1487. doi: [10.1002/joc.3777](https://doi.org/10.1002/joc.3777)
- Mock SJ** (1966) Fluctuations of the terminus of the Harald Moltke Bræ, Greenland. *Journal of Glaciology* **6**(45), 369–373. doi: [10.1017/s002214300001947x](https://doi.org/10.1017/s002214300001947x)
- Möller M, Friedl P, Palmer SJ and Marzeion B** (2022) Grounding line retreat and ice discharge variability at two surging, ice shelf-forming basins of Flade Isblink ice cap, northern Greenland. *Journal of Geophysical Research: Earth Surface* **127**(2), e2021JF006302. doi: [10.1029/2021JF006302](https://doi.org/10.1029/2021JF006302)
- Moon T, Joughin I, Smith B and Howat I** (2012) 21st-century evolution of Greenland outlet glacier velocities. *Science* **336**(6081), 576–578. doi: [10.1126/science.1219985](https://doi.org/10.1126/science.1219985)
- Mouginot J and 8 others** (2019) Forty-six years of Greenland ice sheet mass balance from 1972 to 2018. *Proceedings of the National Academy of Sciences* **116**(19), 9239–9244. doi: [10.1073/pnas.1904242116](https://doi.org/10.1073/pnas.1904242116)
- Mouginot J, Björk AA, Millan R, Scheuchl B and Rignot E** (2018) Insights on the surge behavior of Storstrømmen and L. Bistrup Brae, northeast Greenland, over the last century. *Geophysical Research Letters* **45**(20), 11–197. doi: [10.1029/2018GL079052](https://doi.org/10.1029/2018GL079052)
- Mukherjee K and 6 others** (2017) Surge-type glaciers in the Tien Shan (central Asia). *Arctic, Antarctic, and Alpine Research* **49**(1), 147–171. doi: [10.1657/AAAR0016-021](https://doi.org/10.1657/AAAR0016-021)
- Muñoz-Sabater J** (2019) ERA5-Land monthly averaged data from 1981 to present, Copernicus climate change service (C3S) climate data store (CDS) [data set]. doi: [10.24381/cds.68d2bb30](https://doi.org/10.24381/cds.68d2bb30)
- Murray T and 10 others** (2010) Ocean regulation hypothesis for glacier dynamics in southeast Greenland and implications for ice sheet mass changes. *Journal of Geophysical Research: Earth Surface* **115**, F03026. doi: [10.1029/2009JF001522](https://doi.org/10.1029/2009JF001522)
- Murray T and 13 others** (2015) Extensive retreat of Greenland tidewater glaciers, 2000–2010. *Arctic, Antarctic, and Alpine Research* **47**(3), 427–447. doi: [10.1657/AAAR0014-049](https://doi.org/10.1657/AAAR0014-049)
- Murray T, Strozzi T, Luckman A, Jiskoot H and Christakos P** (2003) Is there a single surge mechanism? Contrasts in dynamics between glacier surges in Svalbard and other regions. *Journal of Geophysical Research: Solid Earth* **108** (B5), 2237. doi: [10.1029/2002JB001906](https://doi.org/10.1029/2002JB001906)
- Murray T, Strozzi T, Luckman A, Pritchard H and Jiskoot H** (2002) Ice dynamics during a surge of Sortebræ, east Greenland. *Annals of Glaciology* **34**, 323–329. doi: [10.3189/172756402781817491](https://doi.org/10.3189/172756402781817491)
- Noh MJ and Howat IM** (2015) Automated stereo-photogrammetric DEM generation at high latitudes: surface extraction with TIN-based search-space minimization (SETSM) validation and demonstration over glaciated regions. *GIScience & Remote Sensing* **52**(2), 198–217. doi: [10.1080/15481603.2015.1008621](https://doi.org/10.1080/15481603.2015.1008621)
- Nuth C and 9 others** (2019) Dynamic vulnerability revealed in the collapse of an Arctic tidewater glacier. *Scientific Reports* **9**(1), 1–13. doi: [10.1038/s41598-019-41117-0](https://doi.org/10.1038/s41598-019-41117-0)
- Nuth C and Kääh A** (2011) Co-registration and bias corrections of satellite elevation data sets for quantifying glacier thickness change. *The Cryosphere* **5**(1), 271–290. doi: [10.5194/tc-5-271-2011](https://doi.org/10.5194/tc-5-271-2011)
- Olesen OB and Reeh N** (1969) Preliminary report on glacier observations in Nordvestfjord, east Greenland. *Rapport Grønlands Geologiske Undersøgelse* **21**, 41–53. doi: [10.34194/rapgu.v21.7213](https://doi.org/10.34194/rapgu.v21.7213)
- Palmer SJ, Shepherd A, Sundal A, Rinne E and Nienow P** (2010) InSAR observations of ice elevation and velocity fluctuations at the Flade Isblink ice cap, eastern north Greenland. *Journal of Geophysical Research: Earth Surface* **115**, F04037. doi: [10.1029/2010JF001686](https://doi.org/10.1029/2010JF001686)
- Pellitero R and 8 others** (2015) A GIS tool for automatic calculation of glacier equilibrium-line altitudes. *Computers & Geosciences* **82**, 55–62. doi: [10.1016/j.cageo.2015.05.005](https://doi.org/10.1016/j.cageo.2015.05.005)
- Porter C and 10 others** (2018) ArcticDEM. *Harvard Dataverse*. <https://doi.org/10.7910/DVN/OHHUKH>.
- Post A** (1969) Distribution of surging glaciers in western North America. *Journal of Glaciology* **8**(53), 229–240. doi: [10.3189/S0022143000031221](https://doi.org/10.3189/S0022143000031221)
- Pritchard H, Murray T, Luckman A, Strozzi T and Barr S** (2005) Glacier surge dynamics of Sortebræ, east Greenland, from synthetic aperture radar feature tracking. *Journal of Geophysical Research: Earth Surface* **110**, F03005. doi: [10.1029/2004JF000233](https://doi.org/10.1029/2004JF000233)
- Pritchard H, Murray T, Strozzi T, Barr S and Luckman A** (2003) Surge-related topographic change of the glacier Sortebræ, east Greenland, derived from synthetic aperture radar interferometry. *Journal of Glaciology* **49**(166), 381–390. doi: [10.3189/172756503781830593](https://doi.org/10.3189/172756503781830593)
- Quincey DJ and 5 others** (2011) Karakoram glacier surge dynamics. *Geophysical Research Letters* **38**, L18504. doi: [10.1029/2011GL049004](https://doi.org/10.1029/2011GL049004)
- Rastner P and 5 others** (2012) The first complete inventory of the local glaciers and ice caps on Greenland. *The Cryosphere* **6**(6), 1483–1495. doi: [10.5194/tc-6-1483-2012](https://doi.org/10.5194/tc-6-1483-2012)
- Rau F, Mauz F, Vogt S, Khalsa SJS and Raup B** (2005) Illustrated GLIMS glacier classification manual. Institut für Physische Geographie Freiburg, Germany, and National Snow and Ice Data Center, Boulder, USA, version, 1, 755.
- Rea BR** (2009) Defining modern day area-altitude balance ratios (AABRs) and their use in glacier-climate reconstructions. *Quaternary Science Reviews* **28** (3–4), 237–248. doi: [10.1016/j.quascirev.2008.10.011](https://doi.org/10.1016/j.quascirev.2008.10.011)
- Rea BR and Evans DJA** (2011) An assessment of surge-induced crevassing and the formation of crevasse squeeze ridges. *Journal of Geophysical Research: Earth Surface* **116**, F04005. doi: [10.1029/2011JF001970](https://doi.org/10.1029/2011JF001970)

- Reeh N, Boggild CE and Oerter H (1994) Surge of Storstrømmen, a large outlet glacier from the Inland ice of north-east Greenland. *Rapport Grønlands Geologiske Undersøgelse* **162**, 201–209. doi: [10.34194/rapgg.v162.8263](https://doi.org/10.34194/rapgg.v162.8263)
- Reeh N, Mohr JJ, Madsen SN, Oerter H and Gundestrup NS (2003) Three-dimensional surface velocities of Storstrømmen glacier, Greenland, derived from radar interferometry and ice-sounding radar measurements. *Journal of Glaciology* **49**(165), 201–209. doi: [10.3189/172756503781830818](https://doi.org/10.3189/172756503781830818)
- RGI Consortium (2017) *Randolph Glacier Inventory – A Dataset of Global Glacier Outlines, Version 6. [Greenland Periphery]*. Boulder, CO, USA. NSIDC: National Snow and Ice Data Center. doi: [10.7265/4m1f-gd79](https://doi.org/10.7265/4m1f-gd79)
- Rignot E, Gogineni S, Joughin I and Krabill W (2001) Contribution to the glaciology of northern Greenland from satellite radar interferometry. *Journal of Geophysical Research: Atmospheres* **106**(D24), 34007–34019. doi: [10.1029/2001JD900071](https://doi.org/10.1029/2001JD900071)
- Roberts DH, Yde JC, Knudsen NT, Long AJ and Lloyd JM (2009) Ice marginal dynamics during surge activity, Kuannersuit Glacier, Disko Island, west Greenland. *Quaternary Science Reviews* **28**(3–4), 209–222. doi: [10.1016/j.quascirev.2008.10.022](https://doi.org/10.1016/j.quascirev.2008.10.022)
- Rucklidge J (1966) Observation of hollows in the snow surface of Torv Gletscher, east Greenland. *Journal of Glaciology* **6**(45), 446–449. doi: [10.1017/s0022143000019584](https://doi.org/10.1017/s0022143000019584)
- Rutishauser H (1971) Observations on a surging glacier in east Greenland. *Journal of Glaciology* **10**(59), 227–236. doi: [10.3189/S0022143000013198](https://doi.org/10.3189/S0022143000013198)
- Sevestre H and Benn DI (2015) Climatic and geometric controls on the global distribution of surge-type glaciers: implications for a unifying model of surging. *Journal of Glaciology* **61**(228), 646–662. doi: [10.3189/2015jog14J136](https://doi.org/10.3189/2015jog14J136)
- Sevestre H, Benn DI, Hulton NR and Bælum K (2015) Thermal structure of Svalbard glaciers and implications for thermal switch models of glacier surging. *Journal of Geophysical Research: Earth Surface* **120**(10), 2220–2236. doi: [10.1002/2015JF003517](https://doi.org/10.1002/2015JF003517)
- Sharp M (1988) Surging glaciers: geomorphic effects. *Progress in Physical Geography* **12**(4), 533–559.
- Smart IHM (1968) *University of Dundee Scoresby Land Expedition 1968*. Dundee: University of Dundee.
- Solgaard AM and 7 others (2020) Hagen Bræ: a surging glacier in north Greenland – 35 years of observations. *Geophysical Research Letters* **47**(6), e2019GL085802. doi: [10.1029/2019GL085802](https://doi.org/10.1029/2019GL085802)
- Straneo F and 8 others (2012) Characteristics of ocean waters reaching Greenland's glaciers. *Annals of Glaciology* **53**(60), 202–210. doi: [10.3189/2012AoG60A059](https://doi.org/10.3189/2012AoG60A059)
- Strozzi T, Kääb A and Schellenberger T (2017) Frontal destabilization of Stonebreen, Edgeøya, Svalbard. *The Cryosphere* **11**(1), 553–566. doi: [10.5194/tc-11-553-2017](https://doi.org/10.5194/tc-11-553-2017)
- Sund M, Lauknes TR and Eiken T (2014) Surge dynamics in the Nathorstbreen glacier system, Svalbard. *The Cryosphere* **8**(2), 623–638. doi: [10.5194/tc-8-623-2014](https://doi.org/10.5194/tc-8-623-2014)
- Truffer M and 10 others (2021) Glacier surges. In Haeberli W, Whiteman CA and Shroder JF (eds), *Snow and Ice-Related Hazards, Risks, and Disasters*. Amsterdam, The Netherlands: Elsevier, pp. 417–466. doi: [10.1016/B978-0-12-817129-5.00003-2](https://doi.org/10.1016/B978-0-12-817129-5.00003-2)
- Walsh KM, Howat IM, Ahn Y and Enderlin EM (2012) Changes in the marine-terminating glaciers of central east Greenland, 2000–2010. *The Cryosphere* **6**(1), 211–220. doi: [10.5194/tc-6-211-2012](https://doi.org/10.5194/tc-6-211-2012)
- Weidick A (1984) Location of two glacier surges in west Greenland. *Rapport Grønlands Geologiske Undersøgelse* **120**, 100–104. doi: [10.34194/rapgg.v120.7867](https://doi.org/10.34194/rapgg.v120.7867)
- Weidick A (1988) Surging glaciers in Greenland – a status. *Rapport Grønlands Geologiske Undersøgelse* **140**, 106–110. doi: [10.34194/rapgg.v140.8047](https://doi.org/10.34194/rapgg.v140.8047)
- Weidick A (1995) Satellite image atlas of glaciers of the world: Greenland. U.S. Geological Survey Professional Paper **1386-C**, 1–153.
- Weidick A, Boggild CE and Knudsen NT (1992) Glacier inventory and atlas of west Greenland. *Rapport Grønlands Geologiske Undersøgelse* **158**, 1–194. doi: [10.34194/rapgg.v158.8196](https://doi.org/10.34194/rapgg.v158.8196)
- Westergaard-Nielsen A, Karami M, Hansen BU, Westermann S and Elberling B (2018) Contrasting temperature trends across the ice-free part of Greenland. *Scientific Reports* **8**(1), 1–6. doi: [10.1038/s41598-018-19992-w](https://doi.org/10.1038/s41598-018-19992-w)
- Willis MJ and 11 others (2018) Massive destabilization of an Arctic ice cap. *Earth and Planetary Science Letters* **502**, 146–155. doi: [10.1016/j.epsl.2018.08.049](https://doi.org/10.1016/j.epsl.2018.08.049)
- Wong GJ and 5 others (2015) Coast-to-interior gradient in recent northwest Greenland precipitation trends (1952–2012). *Environmental Research Letters* **10**(11), 114008. doi: [10.1088/1748-9326/10/11/114008](https://doi.org/10.1088/1748-9326/10/11/114008)
- Woodward J, Carver S, Kunzendorf H and Bennike O (2002) Observations of surge periodicity in east Greenland using molybdenum records from marine sediment cores. *Geological Society, London, Special Publications* **203**(1), 367–373. doi: [10.1144/gsl.sp.2002.203.01.19](https://doi.org/10.1144/gsl.sp.2002.203.01.19)
- Wytiahlowsky HE, Stokes CR and Evans DJA (2023) Remote sensing of glacier change (1965–2021) and identification of surge-type glaciers on Severnaya Zemlya, Russian High Arctic. *Journal of Glaciology*.
- Yde JC and 5 others (2019) Kuannersuit glacier revisited: constraining ice dynamics, landform formations and glaciomorphological changes in the early quiescent phase following the 1995–98 surge event. *Geomorphology* **330**, 89–99. doi: [10.1016/j.geomorph.2019.01.012](https://doi.org/10.1016/j.geomorph.2019.01.012)
- Yde JC and Knudsen NT (2005) Glaciological features in the initial quiescent phase of Kuannersuit Glacier, Greenland. *Geografiska Annaler: Series A, Physical Geography* **87**(3), 473–485. doi: [10.1111/j.0435-3676.2005.00272.x](https://doi.org/10.1111/j.0435-3676.2005.00272.x)
- Yde JC and Knudsen NT (2007) 20th-century glacier fluctuations on Disko Island (Qeqertarsuaq), Greenland. *Annals of Glaciology* **46**, 209–214. doi: [10.3189/172756407782871558](https://doi.org/10.3189/172756407782871558)